POWER FLOW ANALYSIS WITH UNIFIED POWER FLOW CONTROLLER

Dissertation submitted in partial fulfillment of the requirements for the award of degree of

Master of Engineering

in

Power Systems & Electric Drives

By:

Adit Pandita

(Roll. No. 801141001)

Under the supervision of:

Dr. Sanjay K. Jain

Associate Professor, EIED

ELECTRICAL AND INSTRUMENTATION ENGINEERING DEPARTMENT

THAPAR UNIVERSITY

PATIALA – 147004

JULY, 2013

CERTIFICATE

I hereby certify that the work which is being presented in the dissertation entitled, **"Power Flow Analysis with Unified Power Flow Controller"**, in partial fulfillment of the requirements for the award of degree of Master of Engineering in Power Systems and Electric Drives submitted in Electrical and Instrumentation Engineering Department of Thapar University, Patiala is an authentic record of my own work carried out under the supervision of Dr. Sanjay K. Jain, Associate Professor, EIED.

The matter presented in this dissertation has not been submitted for the award of any other degree of this or any other university.

(Adit Pandita)

Roll. No. - 801141001

This is to certify that the above statement made by the candidate is correct and true to best of my knowledge.

(Dr. Sanjay K. Jain)
12/07/2013
Associate Professor
EIED, Thapar University

Countersigned by:

(Dr. S. Ghosh)
Professor & Head, EIED
Thapar University

(Dr. S. K. Mohapatra)
Sr. Professor & Dean (Academic Affairs)
Thapar University

ACKNOWLEDGEMENT

I feel honored in expressing my profound sense of gratitude and indebtedness to **Dr. Sanjay K. Jain**, Associate Professor, EIED, Thapar University, Patiala for his guidance, meticulous efforts, constructive criticism, inspiring encouragement, unflinching support and invaluable co-operation which enabled me to enrich my knowledge and reproduce it in the present form.

I also like to extend my gratefulness to **Dr. S. Ghosh**, Professor & Head, **Ms. Manbir Kaur**, Associate Professor & P.G. Coordinator (Power Systems & Electric Drives), EIED, Thapar University, Patiala for their perpetual encouragement, generous help and inspiring guidance.

I am also very thankful to the entire faculty and staff members of EIED for their direct–indirect help, cooperation, love and affection, which made my stay at Thapar University memorable.

I am very grateful to my parents for their constant support and love to carry out my work effectively.

I also wish to thank all my classmates for their time to time suggestions and cooperation without which I would not have been able to complete my work.

(Adit Pandita)

Roll. No. - 801141001

ABSTRACT

Flexible Alternating Current Transmission Systems (FACTS) have been proposed as an effective solution for controlling power flow and regulating bus voltage in electrical power systems. The use of FACTS is also intended to increase transfer capability, reduce losses, and improved stability. Unified Power Flow Controller (UPFC) is the most promising and effective FACTS system for power flow control.

Various steady state models of UPFC that are suitable for incorporation in power flow programs are analyzed. The Comprehensive NR model of the UPFC is realized in MATLAB program. The power flow solution is based on Newton-Raphson method. The effectiveness of UPFC is studied on 5-Bus Test system. The UPFC is operated to control voltage magnitude and the line flow. The effect of UPFC placement has been studied. The effect of initial voltage of converter, the effect of converter reactance has been studied on power flow convergence.

TABLE OF CONTENTS

LIST OF FIGURES

LIST OF TABLES

CHAPTER – 1

INTRODUCTION

1.1 OVERVIEW

The increasing Industrialization and urbanization of life style has led to increasing dependency on the electrical energy. This has resulted into rapid growth of power systems. This rapid growth has resulted into few uncertainties. Power disruptions and individual power outages are among the major problems. In contrast to the rapid changes in technologies and the power required by these technologies, transmission systems are being pushed to operate closer to their stability limits. The major problems faced by power industries in establishing the match between supply and demand are:

- Supply the electric demand without exceeding the thermal limit.
- Avoid power disruptions and blackouts arising due to stability problem to avoid huge losses.

The concept of Flexible AC Transmission Systems (FACTS) was first defined by N.G. Hingorani, in 1988 [1]. Flexible AC Transmission Systems (FACTS) devices can enhance transmission system control capability and thereby the line loading can be increased in some cases all the way up to thermal limits without compromising reliability. These devices can be an alternative to reduce the flows in heavily loaded lines, resulting in an increased loadability, low system loss, improved stability of the network, reduced cost of production and fulfilled contracture requirement by controlling the power flows in the network, reduce cost of production and fulfilled contracture requirement by controlling the power flows in the network. These capabilities allow transmission system owners and operators to maximize asset utilization and execute additional bulk transfer with immediate bottom-line benefits.

The FACTS provides higher controllability in power systems by means of power electronic devices. Several FACTS-devices have been introduced for various applications worldwide. In most of the applications, the controllability is used to avoid cost intensive or

landscape requiring extensions of power systems, for instance like upgrades or additions of substations and power lines. The FACTS-devices provide a better adaptation to varying operational conditions and improve the usage of existing installations. FACTS devices provide new control facilities, both in steady state power control and dynamic stability control.

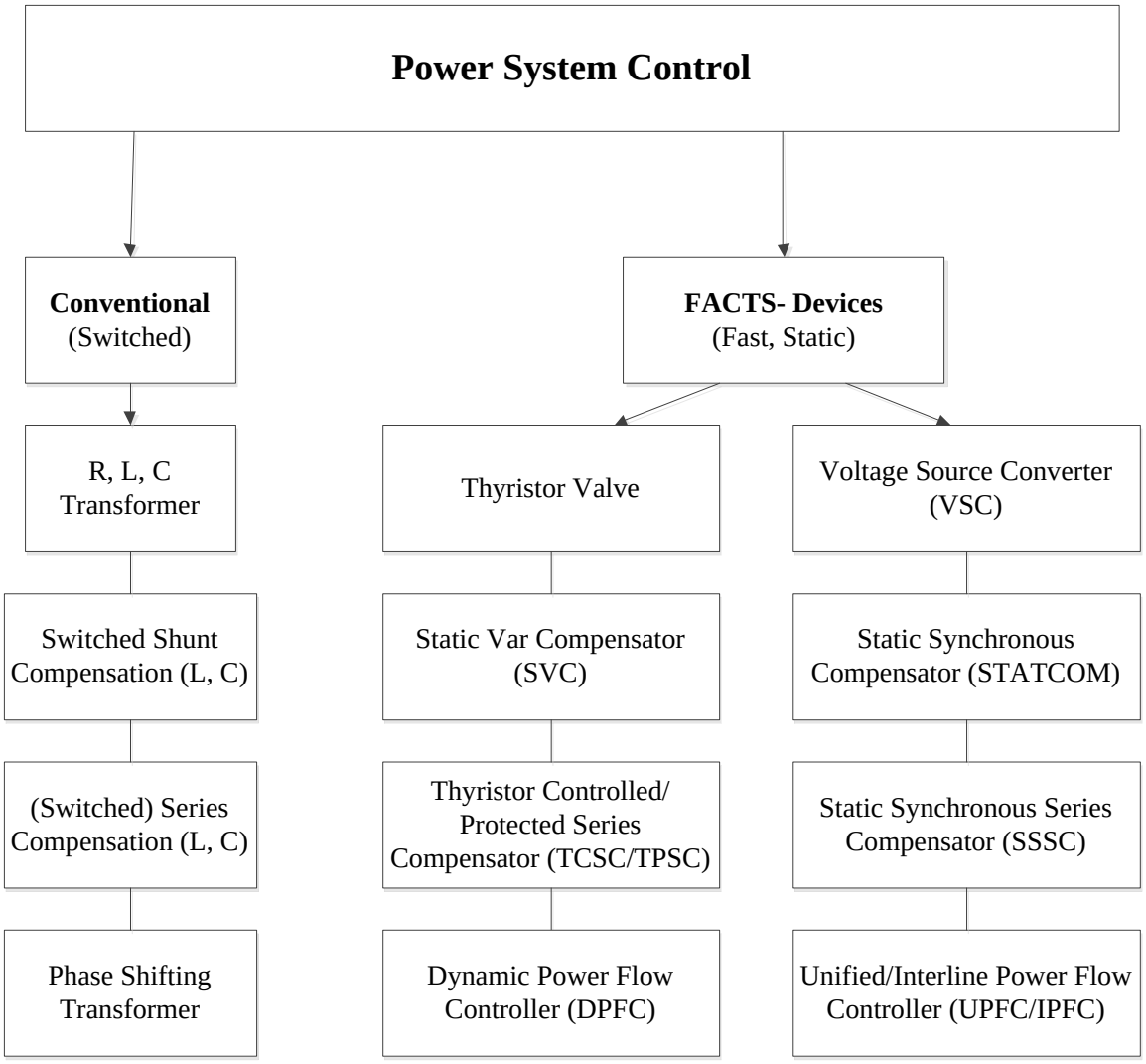

Fig. 1.1 Classification of major FACTS Devices

FACTS mainly find applications in the following areas:

- Power transmission
- Power quality
- Railway grid connection

- Wind power grid connection
- Cable systems

With FACTS, the following benefits can be attained in AC systems:

- Improved power transmission capability
- Improved system stability and availability
- Improved power quality
- Minimized environmental impact
- Minimized transmission losses

The Fig. 1.1 depicts the classifications of various controllable systems including FACTS used in a power system network.

The Unified Power Flow Controller (UPFC) is, arguably, the most comprehensive device from the FACTS initiative. The UPFC is capable of providing active and reactive power control, as well as adaptive voltage magnitude control. The UPFC can independently or simultaneously control the active power, reactive power, and the bus voltage to which it is connected. This controller offers substantial advantages for the static and dynamic operation of power system. The allocation of the UPFC for purposes like reduction in losses, bus voltage support, controlling the power flow through a line can be decided by power flow solutions. This controller also helps in increasing the loadability of the power system and providing better security and reliability to a power system network. It also helps in providing better voltage stability by setting appropriate control parameters.

Power flow calculations are performed in power systems for planning, operational planning, and operation/control. Power flow equations, commonly referred to as power flow are the backbone of power system analysis and design. The power flow problem consists of the calculation of power flows and voltages of a network for a specified terminal or bus conditions. Appropriate steady state model of power system is needed for writing the computer programs. The model includes non-linear algebraic equations, which must be solved iteratively. Power flow calculations are needed for both steady state analysis and initializations of different dynamic analysis.

1.2 LITERATURE REVIEW

In past, researchers have used various techniques in power flow studies to incorporate UPFC to minimize losses, generation costs and maximize loadability, social welfare etc. A brief review on power flow analysis UPFC and its applicability is presented here.

Fuerte-Esquivel and Acha [2] proposed a new and comprehensive UPFC model which is incorporated into an existing FACTS Newton- Raphson load flow algorithm. Critical comparisons are made against existing UPFC models, which show the newly developed model to be far more flexible and efficient.

Lim *et al*. [3] presented UPFC operation for minimization of delivery cost and power production in normal operation state. The delivery cost due to transmission loss is minimized by active power control of UPFC using uncoupled model of UPFC in power flow.

Ambriz-Perez *et al.* [4] addressed the issue of Unified Power Flow Controller (UPFC) modeling within the context of Optimal Power Flow (OPF) solutions. The nonlinear optimization problem is solved by Newton's method. The solution with several UPFCs can be obtained with equal reliability.

Nabavi-Niaki and Iravani [5] outlined an approach for mathematical modeling of unified power flow controller (UPFC) and develop steady-state model, small-signal (linearized) dynamic model, and state-space, large-signal model of UPFC.

Fuerte-Esquivel *et al.* [6] presented a model which is incorporated into an existing Newton-Raphson load flow algorithm. The model can be set to control active and reactive powers and voltage magnitude in any combination. A set of analytical equations has been derived to provide initial conditions. The guidelines are suggested for control coordination between two or more UPFCs.

Radman and Raje [7] presented procedure for steady state power flow calculation of power systems with multiple flexible AC transmission system (FACTS) controllers. Three FACTS controllers namely (STATic synchronous COMpensator (STATCOM), Static Synchronous Series Compensator (SSSC), and Unified Power Flow Controller (UPFC) are studied. Newton–Raphson method of iterative solution is used for power flow equations in polar

coordinate. The impacts of FACTS controllers on power flow are accommodated by adding new entries and modifying some existing entries in the linearized Jacobian equation of the same system with no FACTS controllers.

Santos *et al.* [8] outlined a model suitable for including UPFC devices in steady state studies. The proposed model is able to preserve the traditional Newton-Raphson technique. The model allows easy incorporation of UPFC and automatic UPFC parameters calculation and takes into account the existence of operating limits that cannot be violated

Abdelsalam *et al.* [9] outlined an algorithm to find the optimal location of the Unified Power Flow Controller in electrical power systems. The algorithm utilizes the steady state injection model of UPFC, a continuation power flow and an optimal power flow. The problem is formulated to find the location of UPFC in order to minimize the generation cost function and the investment on the UPFC device.

Farhangfar *et al.* [10] presented an injection model of UPFC to investigate its effect on power flow and loss reduction in power system. The location of UPFC for loss reduction is obtained by two methods. The first method increases transmission power in lines with low impedances and the second method increases the transmission power in transmission lines with impedances.

Chen *et al.* [11] discussed control of UPFC to improve power system voltage stability with dynamical UPFC model. The impact of the UPFC model on voltage stability is clarified through bifurcation analysis and these techniques are employed for the series and shunt branches control and the DC capacitor voltage control

Yap *et al.* [12] presented an effective utilization of UPFC in power flow control to improve existing transmission capability of the power system network. The analysis between UPFC and HVDC (High Voltage Direct Current) is presented for comparison in power quality and cost efficiency.

Mokhlis *et al.* [13] described the implementation of Unified Power Flow Controller (UPFC) steady-state model into Fast Decoupled load flow analysis. The model is integrated through sequential approach, where equations for solving these devices are separated from the basic Fast Decoupled equations

Singh *et al.* [14] suggested the suitable locations of UPFC to enhance system loadability. A sensitivity based approach has been developed for finding suitable placement of UPFC. The optimal power flow problem involves a nonlinear objective function and a set of nonlinear equality and inequality constraints. Sequential Quadratic Programming (SQP) has been used to obtain OPF solutions.

Kim *et al.* [15] presented a new UPFC operation algorithm to find the operating point of UPFCs for the system security level Enhancement. The algorithm iteratively minimizes the security index which indicates the overload level of transmission lines. This method provides relief from congestion to normal operating system and also enlarges security margin to prevent overload problem of the system during faulted condition.

Shaheen *et al.* [16] presented two Evolutionary Optimization Techniques, namely Genetic Algorithm (GA) and Particle Swarm Optimization (PSO) to select the optimal location and the optimal parameters setting of UPFC which minimize the active power losses in the power network, and compare their performances.

1.3 OBJECTIVE OF WORK

The work in this dissertation has been carried out with the objective of studying the UPFC models which can be incorporated in Power Flow solutions. The work is also carried out with the objective to investigate the effect of UPFC parameters and its effectiveness in power system for voltage support and loss minimization by simulating the comprehensive NR model in power flow.

1.4 ORGANIZATION OF DISSERTATION

The dissertation is organized into five chapters. The organization of dissertation is as follows:

The Chapter-1 highlights the brief overview, summary of work carried out by various researchers, the objective of the dissertation and the outline of the dissertation.

The Chapter- 2 presents the overview of UPFC and a comparative study of various steady state models of UPFC with power flow studies has been shown.

The Chapter-3 presents the review on conventional Power Flow Analysis by Newton Raphson method. It also explores the incorporation of Comprehensive Newton Raphson UPFC model into Power Flow Studies and is depicted by flowchart as well.

The Chapter-4 summarizes the effects of UPFC when placed at various locations in a 5-Bus test network on voltage regulation and active and reactive power flows in the transmission lines.

The Chapter-5 summarizes the conclusion drawn after the study and lists the scope for further work.

CHAPTER – 2

UPFC MODELS FOR POWER FLOW STUDIES

2.1 STEADY STATE MODELS OF UPFC

The UPFC is a combination of a static shunt compensator and static series compensator. It acts as a shunt compensating and a phase shifting device simultaneously. The UPFC utilizes a shunt and a series transformer, which are used to connect two voltage source converters with a common DC-capacitor. The DC-circuit allows the active power exchange between shunt and series transformer to control the phase shift of the series voltage. This setup, as shown in Fig.3.1, provides the full controllability for voltage and power flow. The series converter needs to be protected with a Thyristor bridge. Due to the high efforts for the Voltage Source Converters and the protection, an UPFC is getting quite expensive, which limits the practical applications where the voltage and power flow control is required simultaneously.

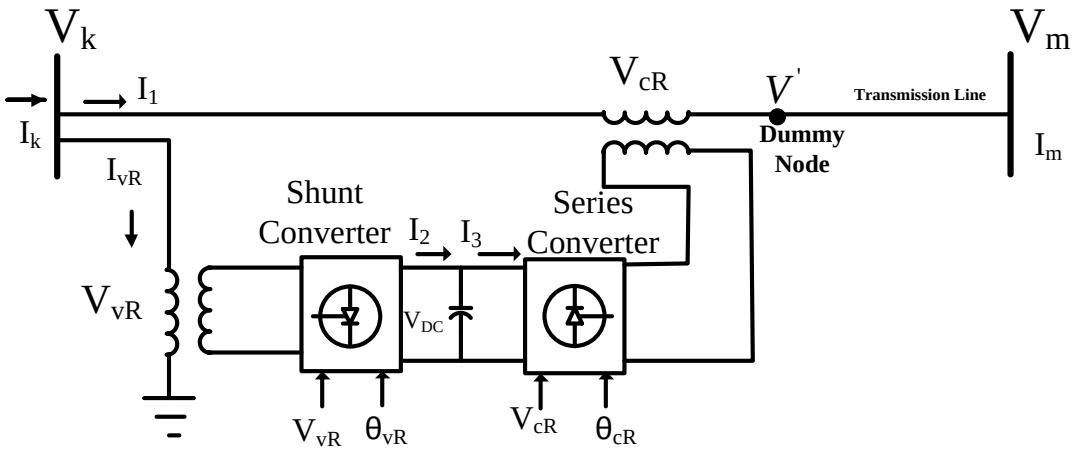

Fig. 2.1: UPFC Schematic diagram

The UPFC is a FACTS device which is capable of providing active and reactive load flow control between its terminals. It may also provide reactive power compensation to the bus at which it is connected. The device consists of two converters connected together by a common

DC link as shown in Fig. 3.1. These converters are connected to the power system via coupling transformers. One converter is connected in shunt to the sending end bus while the second converter is connected in series between the sending and receiving end bus. The UPFC cannot generate or absorb active power and as such the active power in the two converters must be balanced when active power loss is neglected. This is achieved via the DC link. The converters, however, may generate or absorb reactive power.

There are various techniques for inclusion of steady state models of the UPFC in power flow programs. The four techniques that have been used for incorporating UPFC in power flow and their comparative study is presented herewith. These techniques are –

- Decoupled model
- Injection model
- Comprehensive NR model
- Synchronous voltage source model

2.2 DECOUPLED MODEL

A sequential UPFC power flow model proposed by Nabavi-Niaki and Iravani [5] is capable of regulating the power flow from bus m to bus k and to regulate the nodal voltage magnitude at bus k. In this situation, assuming a loss free UPFC operation and neglecting the resistance in voltage source impedances, the UPFC and coupling transformers can be modeled by means of a load at bus k and a generator at bus m. This is shown in Fig. 2.2.

The sending end of UPFC is transformed into a PQ bus, while the receiving end is transformed into PV bus. The active and reactive power loads in PQ bus are set to the values being controlled by UPFC. The standard power flow solution is carried out with an equivalent model given by Fig. 2.2 (b). After power flow convergence a set of non-linear equations is solved by iteration to compute the UPFC parameters.

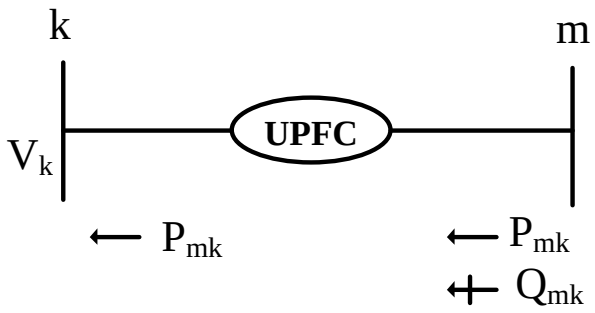

Fig. 2.2 (a): UPFC model

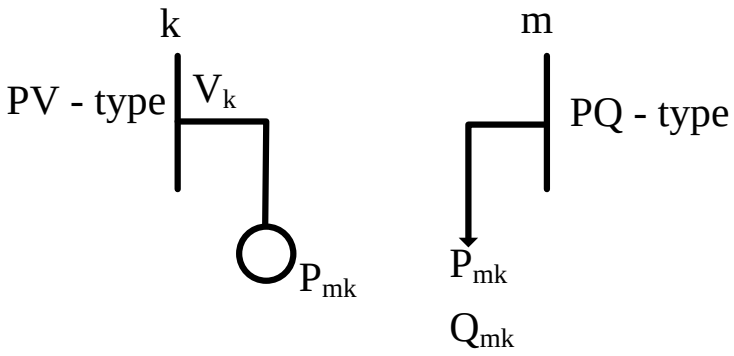

Fig. 2.2 (b): UPFC model equivalent

A) Drawbacks of Decoupled Model

Although this sequential method is simple but it is not clear how the model can be used in situations when the UPFC is not controlling the voltage magnitude, line active power and line reactive power simultaneously. Moreover since UPFC parameters are computed after power flow is converged, however it is not known during this iterative process whether or not the UPFC parameters are within limits. The UPFC parameters are computed iteratively by Newton-Raphson method, no guidelines are given to select suitable UPFC parameters starting values.

2.3 INJECTION MODEL

This model is helpful in understanding the impact of the UPFC on the power system in the steady state. Furthermore, the UPFC injection model can easily be incorporated in the steady state power flow model. Since the series voltage source converter does the main function of the UPFC, it is appropriate to discuss the modeling of a series voltage source converter first.

A) Series Connected Voltage Source Converter Model

Suppose a series connected voltage source is located between bus **i** and **j** in a power system. The series voltage source converter can be modeled with an ideal series voltage $\overrightarrow{V_s}$ in series with a reactance X_s. In Fig. 2.3, $\overrightarrow{V_s}$ models an ideal voltage source and $\overrightarrow{V_i'}$ represents a fictitious voltage behind the series reactance. We have:

$$\overrightarrow{V_i'} = \overrightarrow{V_S} + \overrightarrow{V_i} \tag{2.1}$$

The series voltage source $\overrightarrow{V_s}$ is controllable in magnitude and phase, i.e.:

$$\overrightarrow{V_S} = r\overrightarrow{V_i}e^{j\gamma} \tag{2.2}$$

Where $0 < r < r_{max}$ and $0 < \gamma < 2\pi$.

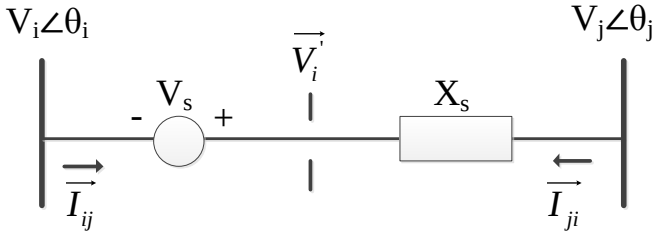

Fig. 2.3: Representation of a series connected VSC

The equivalent circuit vector diagram is shown in Fig. 2.4.

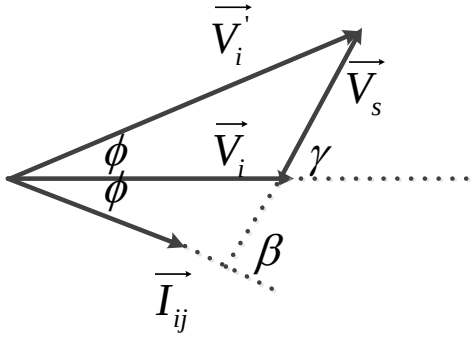

Fig. 2.4: Vector diagram of the equivalent circuit of VSC

The injection model is obtained by replacing the voltage source $\overrightarrow{V_s}$ by the current source $\overrightarrow{I_s} = -jb_s\overrightarrow{V_S}$ in parallel with the line $b_s = \frac{1}{X_s}$.

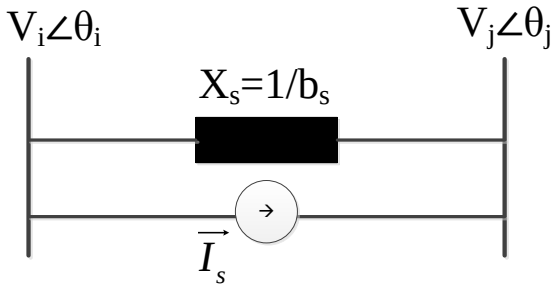

Fig. 2.5: Replacement of a series voltage source by a current source

The current sources $\vec{I}_s$ corresponds to the injection powers $\vec{S}_{is}$ and $\vec{S}_{js}$ where,

$$\vec{S}_{is} = \vec{V}_i(-\vec{I}_s)^* \tag{2.3}$$

$$\vec{S}_{js} = \vec{V}_j(-\vec{I}_s)^* \tag{2.4}$$

The injection power $\vec{S}_{is}$ and $\vec{S}_{js}$ are simplified to:

$$\vec{S}_{is} = \vec{V}_i[\mathrm{jb_s r}\vec{V}_i\, \mathrm{e}^{j\gamma}]^* = -b_s r V_i^2 \sin\gamma - jb_s r V_i^2 \cos\gamma \tag{2.5}$$

If we define: $\theta_{ij} = \theta_i - \theta_j$, we have:

$$\vec{S}_{js} = \vec{V}_j[-\mathrm{jb_s r}\vec{V}_j\, \mathrm{e}^{j\gamma}]^* = b_s r V_i\, \mathrm{V}_j \sin(\theta_{ij}+\gamma) + jb_s r V_i\, \mathrm{V}_j \cos(\theta_{ij}+\gamma) \tag{2.6}$$

Based on the explanation above, the injection model of a series connected voltage source can be seen as two dependent loads as shown in Fig. 2.6.

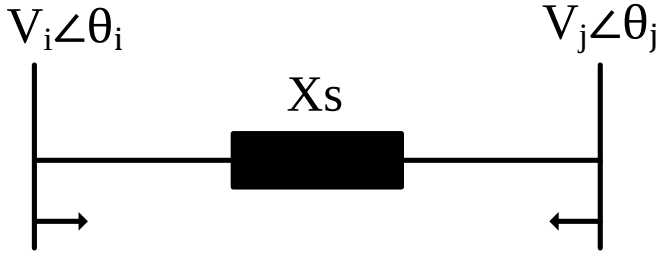

$$P_{si} = rb_s V_i^2 \sin\gamma \qquad P_{sj} = -rb_s V_i\, \mathrm{V}_j \sin(\theta_{ji}+\gamma)$$

$$Q_{si} = rb_s V_i^2 \cos\gamma \qquad Q_{sj} = -rb_s V_i\, \mathrm{V}_j \cos(\theta_{ji}+\gamma)$$

Fig. 2.6: Injection model for a series connected VSC

B) UPFC Model

Reference [17] presents an approach of modeling the UPFC as a series fixed reactance X_s together with a set of active and reactive nodal power injections at each end of the series reactance P_{si}, Q_{si}, P_{sj}, Q_{sj}. These powers are expressed as a function of the terminal, nodal voltages, and a voltage of a series source, which represents the UPFC series converter. The Fig. 2.7 shows complete injection model of UPFC connected between buses i and j. The series voltage source V_{ser} is taken equal to $rVi\angle\gamma$ where $0 < r < r_{max}$ and $o < \gamma < 2\pi$. r and γ represent the control parameters of UPFC.

The UPFC injection model is implemented into a full Newton-Raphson power flow program by adding the UPFC power injections and their derivatives with respect to the AC network state variables, i.e., nodal voltage magnitude and angles, at the appropriate locations in the mismatch vector and Jacobian matrix. The original dimensions of the mismatch vector and Jacobian matrix are not altered at all.

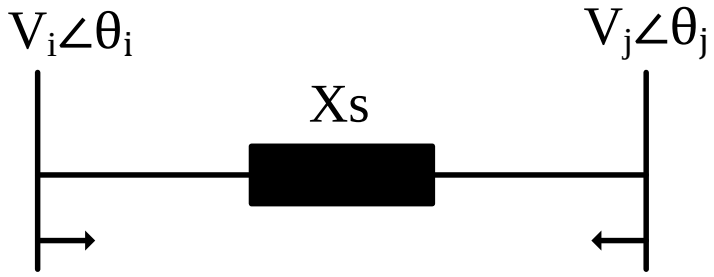

$$P_{si} = rb_s V_i V_j \sin(\theta_{ij} + \gamma) \qquad P_{sj} = -rb_s V_i V_j \sin(\theta_{ij} + \gamma)$$

$$Q_{si} = rb_s V_i^2 \cos\gamma \qquad Q_{sj} = -rb_s V_i V_j \cos(\theta_{ij} + \gamma)$$

Fig. 2.7: UPFC Injection model

C) Merits and Demerits of UPFC Injection Model

The attraction of this formulation is that it can be implemented easily in existing power flow program and UPFC can be adjusted to work as a voltage regulator, series compensator or phase shifter.

The major drawback of this model is that all important aspect of the automatic UPFC parameter adjustment has not been addressed. Also the series voltage course parameters are adjusted by trial and error in order to achieve certain power flow solution, which will match the target power flow.

2.4 COMPREHENSIVE NR MODEL

Trying to overcome the limitations in the decoupled and injection UPFC model, a comprehensive UPFC model is given in paper [2]. This model is straightforward extension of the power flow equations and hence, it is suitable for incorporation into an existing Newton-Raphson power flow algorithm.

This model has been presented in this dissertation report and has been extensively discussed with UPFC model incorporation in power flow studies. This model has been summarized in detail in chapter-3.

A) Merits and Demerits of Comprehensive NR Model

The main advantage of this UPFC model over the Decoupled and injection model is that UPFC state variables are incorporated inside the Jacobian and mismatch equations leading to very robust iterative solution. In this unified solution, the UPFC state variables are adjusted simultaneously with the nodal network state variables in order to achieve the specified control targets. Hence, the interaction between the network and UPFC is better represented and the UPFC state variables can be identified inside the power flow program. This model also gives the ability to control the active and reactive power simultaneously as well as the voltage magnitude. The losses of the UPFC coupling transformers are taken into consideration.

The drawback of this model is that the UPFC does not work in impedance compensation, and phase shift mode. Moreover, the model needs good initial conditions for UPFC state variables for better convergence. Bad initial conditions may cause divergence.

2.5 SYNCHRONOUS VOLTAGE SOURCE MODEL

In this model the shunt converter can be assumed to operate at unity power factor and the UPFC is well represented by an ideal series voltage source, termed synchronous voltage source. The SVS injects a series variable voltage magnitude and angle. These parameters adjust automatically so as to control the active and reactive powers exchanged between the UPFC and the AC system.

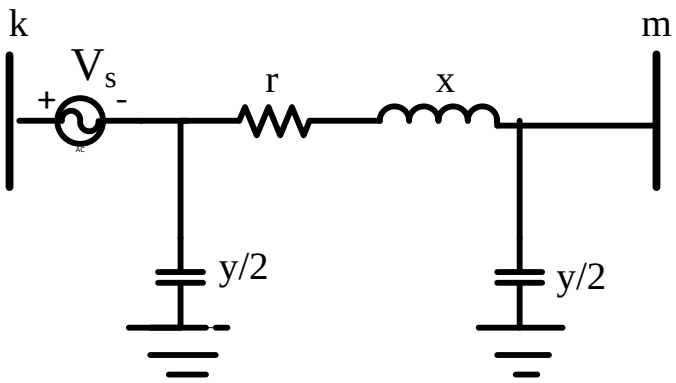

Fig. 2.8: Transmission line Compensated by SVS

The schematic representation of a transmission line compensated by a SVS is given in Fig. 2.8. The complex voltage injected by the SVS source has magnitude V_s ($V_{smin} < V_s < V_{smax}$) variable phase angle θ_s ($0 < \theta_s < 2\pi$).

The general power flow equations for the compensated transmission line are:

At bus k,

$$P_k = V_k^2 G_{kk} + V_k V_m (G_{km} \cos(\theta_k - \theta_m) + B_{km} \sin(\theta_k - \theta_m)) - V_k V_s (G_{kk} \cos(\theta_k - \theta_s) + B_{kk} \sin(\theta_k - \theta_s)) \quad (2.7)$$

$$Q_k = -V_k^2 B_{kk} + V_k V_m (G_{km} \sin(\theta_k - \theta_m) - B_{km} \cos(\theta_k - \theta_m)) - V_k V_s (G_{kk} \sin(\theta_k - \theta_s) - B_{kk} \cos(\theta_k - \theta_s)) \tag{2.8}$$

At bus m,

$$P_m = V_m^2 G_{mm} + V_k V_m (G_{mk} \cos(\theta_m - \theta_k) + B_{mk} \sin(\theta_m - \theta_k)) - V_m V_s (G_{mm} \cos(\theta_m - \theta_s) + B_{mk} \sin(\theta_m - \theta_s)) \tag{2.9}$$

$$Q_m = -V_m^2 B_{mm} + V_m V_k (G_{mk} \sin(\theta_m - \theta_k) - B_{mk} \cos(\theta_m - \theta_k)) - V_m V_s (G_{mk} \sin(\theta_m - \theta_s) - B_{mk} \cos(\theta_m - \theta_s)) \tag{2.10}$$

The linearized Newton equations of the compensated transmission line are given in eqn. (2.11), where the variable phase angle θ_s, and variable magnitude V_s, are taken to be the state variables.

$$\begin{bmatrix} \Delta P_k \\ \Delta P_m \\ \Delta Q_k \\ \Delta Q_m \\ \Delta P_{km} \\ \Delta Q_{km} \end{bmatrix} = \begin{bmatrix} \frac{\partial P_k}{\theta_k} & \frac{\partial P_k}{\theta_m} & \frac{\partial P_k}{V_k} V_k & \frac{\partial P_k}{V_m} V_m & \frac{\partial P_k}{\theta_s} & \frac{\partial P_k}{V_s} V_s \\ \frac{\partial P_m}{\theta_k} & \frac{\partial P_m}{\theta_m} & \frac{\partial P_m}{V_k} V_k & \frac{\partial P_m}{V_m} V_m & \frac{\partial P_m}{\theta_s} & \frac{\partial P_m}{V_s} V_s \\ \frac{\partial Q_k}{\theta_k} & \frac{\partial Q_k}{\theta_m} & \frac{\partial Q_k}{V_k} V_k & \frac{\partial Q_k}{V_m} V_m & \frac{\partial Q_k}{\theta_s} & \frac{\partial Q_k}{V_s} V_s \\ \frac{\partial Q_m}{\theta_k} & \frac{\partial Q_m}{\theta_m} & \frac{\partial Q_m}{V_k} V_k & \frac{\partial Q_m}{V_m} V_m & \frac{\partial Q_m}{\theta_s} & \frac{\partial Q_m}{V_s} V_s \\ \frac{\partial P_{km}}{\theta_k} & \frac{\partial P_{km}}{\theta_m} & \frac{\partial P_{km}}{V_k} V_k & \frac{\partial P_{km}}{V_m} V_m & \frac{\partial P_{km}}{\theta_s} & \frac{\partial P_{km}}{V_s} V_s \\ \frac{\partial Q_{km}}{\theta_k} & \frac{\partial Q_{km}}{\theta_m} & \frac{\partial Q_{km}}{V_k} V_k & \frac{\partial Q_{km}}{V_m} V_m & \frac{\partial Q_{km}}{\theta_s} & \frac{\partial Q_{km}}{V_s} V_s \end{bmatrix} \begin{bmatrix} \Delta\theta_k \\ \Delta\theta_m \\ \Delta\theta_k \\ \Delta\theta_m \\ \Delta\theta_{km} \\ \Delta\theta_{km} \end{bmatrix} \tag{2.11}$$

CHAPTER - 3

COMPREHENSIVE NR UPFC MODEL

3.1 CONVENTIONAL POWER FLOW ANALYSIS

Power flow analysis is probably the most important of all network calculations since it concerns the network performance in its normal operating conditions. It is performed to investigate the magnitude and phase angle of the voltage at each bus and the real and reactive power flows in the system components. Power flow analysis has a great importance in future expansion planning, in stability studies and in determining the best economical operation for existing systems. Also load flow results are very valuable for setting the proper protection devices to insure the security of the system. In order to perform a load flow study, full data must be provided about the studied system, such as connection diagram, parameters of transformers and lines, rated values of each equipment, and the assumed values of real and reactive power for each load. The principle information obtained from a power-flow study is the magnitude and phase angle of the voltage at each bus and the real and reactive power flowing in each line.

Both the bus self- and mutual admittances which compose the bus admittance matrix Y_{bus} or the driving point and transfer impedance which compose Z_{bus} may be used in solving the power-flow problem.

3.1.1 BUS CLASSIFICATION

Each bus in the system has four variables: voltage magnitude, voltage angle, real power and reactive power. During the operation of the power system, each bus has two known variables and two unknowns. Generally, the bus must be classified as one of the following bus types:

A) Slack or Swing Bus

This bus is considered as the reference bus. It must be connected to a generator of high rating relative to the other generators. During the operation, the voltage of this bus is always

specified and remains constant in magnitude and angle. In addition to the generation assigned to it according to economic operation, this bus is responsible for supplying the losses of the system.

B) Generator or Voltage Controlled Bus

During the operation the voltage magnitude at this the bus is kept constant. Also, the active power supplied is kept constant at the value that satisfies the economic operation of the system. Sometimes, this bus is connected to a VAR device where the voltage can be controlled by varying the value of the injected VAR to the bus.

C) **Load Bus**

This bus is not connected to a generator so that neither its voltage nor its real power can be controlled. On the other hand, the load connected to this bus will change the active and reactive power at the bus in a random manner. To solve the load flow problem we have to assume the complex power value (real and reactive) at this bus.

3.1.2 REAL AND REACTIVE POWER INJECTION AT BUS

For the formulation of the real and reactive power entering a bus, we need to define the following quantities. Let the voltage at the i^{th} bus be denoted by

$$V_i = |V_i| \angle \delta_i = |V_i| (\cos \delta_i + j \sin \delta_i) \tag{3.1}$$

Also let us define the self-admittance at bus-*i* as

$$Y_{ii} = |Y_{ii}| \angle \theta_{ii} = |Y_{ii}| (\cos \theta_{ii} + j \sin \theta_{ii}) = G_{ii} + jB_{ii} \tag{3.2}$$

Similarly the mutual admittance between the buses *i* and *j* can be written as

$$Y_{ij} = |Y_{ij}| \angle \theta_{ij} = |Y_{ij}| (\cos \theta_{ij} + j \sin \theta_{ij}) = G_{ij} + jB_{ij} \tag{3.3}$$

Let the power system contains a total number of *n* buses. The current injected at bus-*i* is given as

$$\begin{aligned} I_i &= Y_{i1}V_1 + Y_{i2}V_2 + \cdots + Y_{in}V_n \\ &= \sum_{k=1}^{n} Y_{ik}V_k \end{aligned} \tag{3.4}$$

It is to be noted we shall assume the current entering a bus to be positive and that leaving the bus to be negative. As a consequence the power and reactive power entering a bus will also be assumed to be positive. The complex power at bus-*i* is then given by

$$P_i - jQ_i = V_i^* I_i = V_i^* \sum_{k=1}^{n} Y_{ik} V_k$$

$$= |V_i|(\cos\delta_i - j\sin\delta_i)\sum_{k=1}^{n}|Y_{ik}V_k|(\cos\theta_{ik} + j\sin\theta_{ik})(\cos\delta_k + j\sin\delta_k) \quad (3.5)$$

$$= \sum_{k=1}^{n}|Y_{ik}V_iV_k|(\cos\delta_i - j\sin\delta_i)(\cos\theta_{ik} + j\sin\theta_{ik})(\cos\delta_k + j\sin\delta_k)$$

Note that

$$\begin{aligned}&(\cos\delta_i - j\sin\delta_i)(\cos\theta_{ik} + j\sin\theta_{ik})(\cos\delta_k + j\sin\delta_k)\\ &= (\cos\delta_i - j\sin\delta_i)[\cos(\theta_{ik} + \delta_k) + j\sin(\theta_{ik} + \delta_k)]\\ &= \cos(\theta_{ik} + \delta_k - \delta_i) + j\sin(\theta_{ik} + \delta_k - \delta_i)\end{aligned}$$

Therefore substituting in (3.5) we get the real and reactive power as

$$P_i = \sum_{k=1}^{n}|Y_{ik}V_iV_k|\cos(\theta_{ik} + \delta_k - \delta_i) \quad (3.6)$$

$$Q_i = -\sum_{k=1}^{n}|Y_{ik}V_iV_k|\sin(\theta_{ik} + \delta_k - \delta_i) \quad (3.7)$$

Let real and reactive power generated at bus-*i* be denoted by P_{Gi} and Q_{Gi} respectively. Also let us denote the real and reactive power consumed at the i^{th} bus by P_{Li} and Q_{Li} respectively. Then the net real power injected in bus-*i* is

$$P_{i,inj} = P_{Gi} - P_{Li} \quad (3.8)$$

Let the injected power calculated by the load flow program be $P_{i,calc}$. Then the mismatch between the actual injected and calculated values is given by:

$$\Delta P_i = P_{i,inj} - P_{i,calc} = P_{Gi} - P_{Li} - P_{i,calc} \quad (3.9)$$

In a similar way the mismatch between the reactive power injected and calculated values is given by:

$$\Delta Q_i = Q_{i,inj} - Q_{i,calc} = Q_{Gi} - Q_{Li} - Q_{i,calc} \quad (3.10)$$

The purpose of the load flow is to minimize the above two mismatches. It is to be noted that (3.6) and (3.7) are used for the calculation of real and reactive power in (3.9) and (3.10). However since the magnitudes of all the voltages and their angles are not known a priori, an iterative procedure must be used to estimate the bus voltages and their angles in order to calculate the mismatches. It is expected that mismatches ΔP_i and ΔQ_i reduce with each iteration

and the load flow is said to have converged when the mismatches of all the buses become less than a very small number.

3.1.3 NEWTON RAPHSON (NR) METHOD

Taylor's series expansion for a function of two or more variables is the basis for the Newton-Raphson method for solving the power-flow problem.

The Newton-Raphson method is an iterative technique for solving systems of simultaneous equations in the general form:

$$\begin{aligned} f_1(x_1,....x_n,...x_r) &= K_1 \\ f_n(x_1,....x_n,...x_r) &= K_2 \\ f_r(x_1,....x_n,...x_r) &= K_3 \end{aligned} \tag{3.11}$$

where $f_1,....f_n....f_r$ are differentiable functions of the variables $x_1,....x_n$,....x_r and $K_1....K_n....K_r$ are constants. Applied to the load flow problem, the variables are the nodal voltage magnitudes and phase angles, the functions are the relationships between power, reactive power and bus voltages, while the constants are the specified values of power and reactive power at the generator and load bus.

A) Jacobian Matrix

We shall now discuss the formation of the sub matrices of the Jacobian matrix. To do that we shall use the real and reactive power equations of (3.6) and (3.7). Let us rewrite them with the help of (3.2) as

$$P_i = |V_i|^2 G_{ii} + \sum_{\substack{k=1 \\ k\neq i}}^{n} |Y_{ik} V_i V_k| \cos(\theta_{ik} + \delta_k - \delta_i) \tag{3.12}$$

$$Q_i = -|V_i|^2 B_{ii} - \sum_{\substack{k=1 \\ k\neq i}}^{n} |Y_{ik} V_i V_k| \sin(\theta_{ik} + \delta_k - \delta_i) \tag{3.13}$$

The sub matrices are:

$$J_{11}=\begin{bmatrix}\frac{\partial P_2}{\partial \delta_2} & \cdots & \frac{\partial P_2}{\partial \delta_n}\\ \vdots & \ddots & \vdots \\ \frac{\partial P_n}{\partial \delta_2} & \cdots & \frac{\partial P_n}{\partial \delta_n}\end{bmatrix} \tag{3.14}$$

$$J_{12}=\begin{bmatrix}|V_2|\frac{\partial P_2}{\partial |V_2|} & \cdots & |V_{1+n_p}|\frac{\partial P_2}{\partial |V_{1+n_p}|}\\ \vdots & \ddots & \vdots \\ |V_2|\frac{\partial P_n}{\partial |V_2|} & \cdots & |V_{1+n_p}|\frac{\partial P_n}{\partial |V_{1+n_p}|}\end{bmatrix} \tag{3.15}$$

$$J_{21}=\begin{bmatrix}\frac{\partial Q_2}{\partial \delta_2} & \cdots & \frac{\partial Q_2}{\partial \delta_n}\\ \vdots & \ddots & \vdots \\ \frac{\partial Q_{1+n_p}}{\partial \delta_2} & \cdots & \frac{\partial Q_{1+n_p}}{\partial \delta_n}\end{bmatrix} \tag{3.16}$$

$$J_{22}=\begin{bmatrix}|V_2|\frac{\partial Q_2}{\partial |V_2|} & \cdots & |V_{1+n_p}|\frac{\partial Q_2}{\partial |V_{1+n_p}|}\\ \vdots & \ddots & \vdots \\ |V_2|\frac{\partial Q_{1+n_p}}{\partial |V_2|} & \cdots & |V_{1+n_p}|\frac{\partial Q_{1+n_p}}{\partial |V_{1+n_p}|}\end{bmatrix} \tag{3.17}$$

i. Formation of J_{11}

Let us define J_{11} as

$$J_{11}=\begin{bmatrix}L_{22} & \cdots & L_{2n}\\ \vdots & \ddots & \vdots \\ L_{n2} & \cdots & L_{nn}\end{bmatrix} \tag{3.18}$$

It can be seen from (3.14) that M_{ik}'s are the partial derivatives of P_i with respect to δ_k. The derivative P_i (3.14) with respect to k for $i \neq k$ is given by

$$L_{ik}=\frac{\partial P_i}{\partial \delta_k}=-|Y_{ik}V_iV_k|\sin(\theta_{ik}+\delta_k-\delta_i), \quad i \neq k \tag{3.19}$$

Similarly the derivative P_i with respect to k for $i = k$ is given by

$$L_{ii} = \frac{\partial P_i}{\partial \delta_i} = \sum_{\substack{k=1 \\ k \neq i}}^{n} |Y_{ik} V_i V_k| \sin(\theta_{ik} + \delta_k - \delta_i)$$

Comparing the above equation with (3.13) we can write

$$L_{ii} = \frac{\partial P_i}{\partial \delta_i} = -Q_i - |V_i|^2 B_{ii} \tag{3.20}$$

ii. Formation of J_{21}

Let us define J_{21} as

$$J_{21} = \begin{bmatrix} M_{22} & \cdots & M_{2n} \\ \vdots & \ddots & \vdots \\ M_{n_p 2} & \cdots & M_{n_p n} \end{bmatrix} \tag{3.21}$$

It is evident that the elements of J_{21} are the partial derivative of Q with respect to δ. Also we can write

$$M_{ik} = \frac{\partial Q_i}{\partial \delta_k} = -|Y_{ik} V_i V_k| \cos(\theta_{ik} + \delta_k - \delta_i), \quad i \neq k \tag{3.22}$$

Similarly for $i = k$ we have

$$M_{ii} = \frac{\partial Q_i}{\partial \delta_i} = \sum_{\substack{k=1 \\ k \neq i}}^{n} |Y_{ik} V_i V_k| \cos(\theta_{ik} + \delta_k - \delta_i) = P_i - |V_i|^2 G_{ii} \tag{3.23}$$

The last equality of (2.23) is evident from (2.12).

iii. Formation of J_{12}

Let us define J_{12} as

$$J_{12} = \begin{bmatrix} N_{22} & \cdots & N_{2n_p} \\ \vdots & \ddots & \vdots \\ N_{n2} & \cdots & N_{nn_p} \end{bmatrix} \tag{3.24}$$

As evident, the elements of J_{21} involve the derivatives of real power P with respect to magnitude of bus voltage $|V|$. For $i \neq k$, we can write from (3.12)

$$N_{ik} = |V_k| \frac{\partial P_i}{\partial |V_k|} = |Y_{ik} V_i V_k| \cos(\theta_{ik} + \delta_k - \delta_i) = -M_{ik} \quad i \neq k \tag{3.25}$$

For $i = k$ we have

$$N_{ii} = |V_i|\frac{\partial P_i}{\partial |V_i|} = |V_i|\left[2|V_i|G_{ii} + \sum_{\substack{k=1 \\ k\neq i}}^{n} |Y_{ik}V_k|\cos(\theta_{ik} + \delta_k - \delta_i) \right]$$
$$= 2|V_i|^2 G_{ii} + \sum_{\substack{k=1 \\ k\neq i}}^{n} |Y_{ik}V_iV_k|\cos(\theta_{ik} + \delta_k - \delta_i) = 2|V_i|^2 G_{ii} + M_{ii} \quad (3.26)$$

iv. Formation of J_{22}

For the formation of J_{22} let us define

$$J_{22} = \begin{bmatrix} O_{22} & \cdots & O_{2n_p} \\ \vdots & \ddots & \vdots \\ O_{n_p 2} & \cdots & O_{n_p n_p} \end{bmatrix} \quad (3.27)$$

For $i \neq k$ we can write from (2.13)

$$O_{ik} = |V_i|\frac{\partial Q_i}{\partial |V_k|} = -|V_i||Y_{ik}V_iV_k|\sin(\theta_{ik} + \delta_k - \delta_i) = L_{ik}, \quad i \neq k \quad (3.28)$$

Finally for $i = k$ we have

$$O_{ii} = |V_i|\frac{\partial Q_i}{\partial |V_k|} = |V_i|\left[-2|V_i|B_{ii} - \sum_{\substack{k=1 \\ k\neq i}}^{n} |Y_{ik}V_k|\sin(\theta_{ik} + \delta_k - \delta_i) \right]$$
$$= -2|V_i|^2 B_{ii} - \sum_{\substack{k=1 \\ k\neq i}}^{n} |Y_{ik}V_iV_k|\sin(\theta_{ik} + \delta_k - \delta_i) = -2|V_i|^2 B_{ii} - L_{ii} \quad (3.29)$$

We therefore see that once the sub matrices J_{11} and J_{21} are computed, the formation of the sub matrices J_{12} and J_{22} is fairly straightforward. For large system this will result in considerable saving in the computation time.

B) Algorithm to Build Y-Bus

The Y-Bus matrix formation is needed to carry out power flow calculation and the algorithm for making Y-Bus matrix is as follows:

Step 1. Read NL(number of lines); NB(number of buses).

Step 2. Initialise y_{ijo}=0(i=1,2,....,NB; j=1,2,...NB).

Step 3. Set the line number counter i=1.

Step 4. Read the admittance y between buses j to k and shunt admittance y^{sh} between the bus and reference.

SB_i - stores the index 'i' of the j_{th} bus which is linked to the k_{th} bus.

EB_i - stores the index 'i' of the k_{th} bus which is linked to the j_{th} bus.

y_i - admittance between j_{th} and k_{th} buses.

$y_{i(sh)}$ - admittance between the j_{th} and reference buses.

Step 5. Assign the values

$l = SB_i$

$m = EB_i$

$y_{ll(new)} = y_{ll(old)} + y_i + y_{i(sh)}$

$y_{mm(new)} = y_{lmm(old)} + y_i + y_{i(sh)}$

$y_{lm(new)} = y_{lm(old)} - y_i$

$y_{ml(new)} = y_{ml(old)} - y_i$

Step 6. Check $i \geq NL$, if 'yes' then GOTO step 7 else $i = i + 1$ and GOTO step 4 and repeat.

Step 7. Write the matrix and stop.

C) Newton Raphson Algorithm to Perform Power Flow

The following steps are implemented to perform power flow studies using Newton Raphson method:

Step 1. Choose the initial values of the voltage magnitudes $|V|^{(0)}$ of all n_p load buses and $n-1$ angles $\delta^{(0)}$ of the voltages of all the buses except the slack bus.

Step 2. Use the estimated $|V|^{(0)}$ and $\delta^{(0)}$ to calculate a total $n-1$ number of injected real power $P_{calc}^{(0)}$ and equal number of real power mismatch $\Delta P^{(0)}$.

Step 3. Use the estimated $|V|^{(0)}$ and $\delta^{(0)}$ to calculate a total n_p number of injected reactive power $Q_{calc}{}^{(0)}$ and equal number of reactive power mismatch $\Delta Q^{(0)}$.

Step 4. Use the estimated $|V|^{(0)}$ and $\delta^{(0)}$ to formulate the Jacobian matrix $J^{(0)}$.

Step 5. Solve $J\begin{bmatrix} \Delta\delta_2 \\ \vdots \\ \Delta\delta_n \\ \dfrac{\Delta|V_2|}{|V_2|} \\ \vdots \\ \dfrac{\Delta|V_{1+n_p}|}{|V_{1+n_p}|} \end{bmatrix} = \begin{bmatrix} \Delta P_2 \\ \vdots \\ \Delta P_n \\ \Delta Q_2 \\ \vdots \\ \Delta Q_{1+n_p} \end{bmatrix}$ for $\Delta\delta^{(0)}$ and $\Delta|V|^{(0)} \div |V|^{(0)}$.

Step 6. Obtain the updates from

$$\delta^{(1)} = \delta^{(0)} + \Delta\delta^{(0)} \tag{3.30}$$

$$|V|^{(1)} = |V|^{(0)}\left[1 + \frac{\Delta|V|^{(0)}}{|V|^{(0)}}\right] \tag{3.31}$$

Step 7. Check if all the mismatches are below a small number. Terminate the process if yes. Otherwise go back to step-1 to start the next iteration with the updates given by step (5).

3.2 UNIFIED POWER FLOW CONTROLLER MODEL

The basic principle of UPFC operation has been already discussed in Chapter 2. It follows from that discussion that an equivalent circuit consisting of two coordinated synchronous voltage sources should represent the UPFC adequately for the purpose of fundamental frequency steady-state analysis. Such an equivalent circuit is shown in Fig. 3.1.

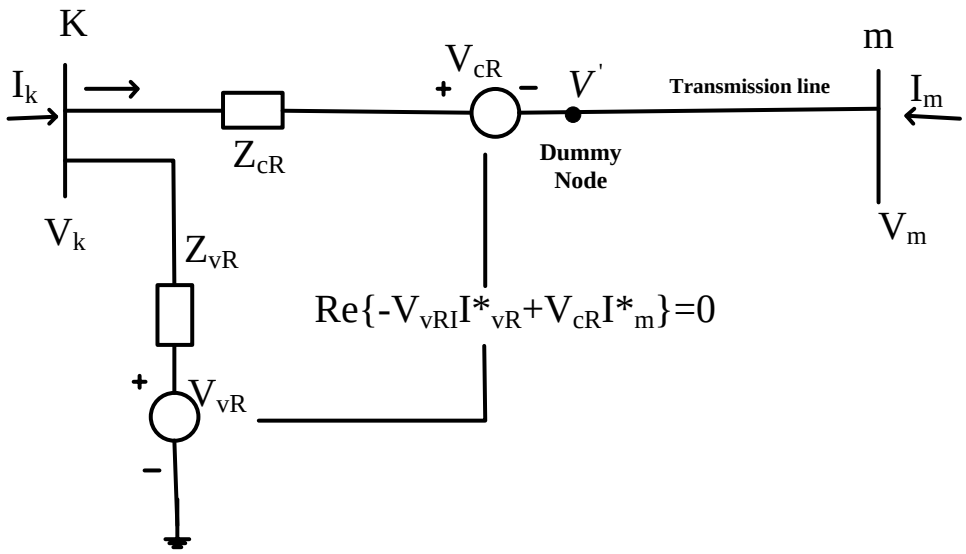

Fig. 3.1: Equivalent Circuit of UPFC

The synchronous voltage sources represent the fundamental Fourier series component of the switched voltage waveforms at the AC converter terminals of the UPFC [1].

The source impedances included in the model represent the positive sequence leakage inductances and resistances of the coupling UPFC transformers. The ideal voltage sources are:

$$V_{vr} = |V_{vr}| \left(cos\theta_{vr} + jsin\theta_{vr}\right) \tag{3.32}$$

$$V_{cr} = |V_{cr}| \left(cos\theta_{cr} + jsin\theta_{cr}\right) \tag{3.33}$$

Here V_{vR} and θ_{vR} are the controllable magnitude $\left(V_{vRmin} \le |V_{vR}| \le V_{vRmax}\right)$ and $\left(0 \le \theta_{vR} \le 2\pi\right)$ phase angle of the voltage source representing the shunt converter. The magnitude V_{cR} and phase angle θ_{cR} of the voltage source representing the series converter are controlled between these limits: $\left(V_{cRmin} \le |V_{cR}| \le V_{cRmax}\right)$ and $\left(0 \le \theta_{cR} \le 2\pi\right)$ respectively.

The phase angle of the series-injected voltage determines the mode of power flow control. If θ_{cR} is in phase with the nodal voltage angle θ_k, the UPFC regulates the terminal voltage. If θ_{cR} is in quadrature with respect to θ_k, it controls active power flow, acting as a phase shifter. If θ_{cR} is in quadrature with the line current angle then it controls active power flow,

acting as a variable series compensator. At any other value of θ_{cR}, the UPFC operates as a combination of voltage regulator, variable series compensator, and phase shifter. The magnitude of the series-injected voltage determines the amount of power flow to be controlled.

3.2.1 UPFC POWER EQUATIONS

Based on equivalent circuit diagram shown in Fig. 3.1, the active and reactive powers are:

At bus k:

$$P_k = V_k^2 G_{kk} + V_k V_m (G_{km}\cos(\theta_k - \theta_m) + B_{km}\sin(\theta_k - \theta_m)) + V_k V_{cR} (G_{km}\cos(\theta_k - \theta_{cR}) + B_{km}\sin(\theta_k - \theta_{cR})) + V_k V_{vR} (G_{vR}\cos(\theta_k - \theta_{vR}) + B_{vR}\sin(\theta_k - \theta_{vR})) \quad (3.34)$$

$$Q_k = -V_k^2 B_{kk} + V_k V_m (G_{km}\sin(\theta_k - \theta_m) - B_{km}\cos(\theta_k - \theta_m)) + V_k V_{cR} (G_{km}\sin(\theta_k - \theta_{cR}) - B_{km}\cos(\theta_k - \theta_{cR})) + V_k V_{vR} (G_{vR}\sin(\theta_k - \theta_{vR}) - B_{vR}\cos(\theta_k - \theta_{vR})) \quad (3.35)$$

At bus m:

$$P_m = V_m^2 G_{mm} + V_m V_k (G_{mk}\cos(\theta_m - \theta_k) + B_{mk}\sin(\theta_m - \theta_k)) + V_m V_{cR} (G_{mm}\cos(\theta_m - \theta_{cR}) + B_{mm}\sin(\theta_m - \theta_{cR})) \quad (3.36)$$

$$Q_m = -V_m^2 B_{mm} + V_m V_k (G_{mk}\sin(\theta_m - \theta_k) - B_{mk}\cos(\theta_m - \theta_k)) + V_m V_{cR} (G_{mm}\sin(\theta_m - \theta_{cR}) - B_{mm}\cos(\theta_m - \theta_{cR})) \quad (3.37)$$

Series converter:

$$P_{cR} = V_{cR}^2 G_{mm} + V_{cR} V_k (G_{km}\cos(\theta_{cR} - \theta_k) + B_{km}\sin(\theta_{cR} - \theta_k)) + V_{cR} V_m (G_{mm}\sin(\theta_{cR} - \theta_m) + B_{mm}\sin(\theta_{cR} - \theta_m)) \quad (3.38)$$

$$Q_{cR} = -V_{cR}^2 B_{mm} + V_{cR} V_k (G_{km} \sin(\theta_{cR} - \theta_k) - B_{km} \cos(\theta_{cR} - \theta_k)) + V_{cR} V_m (G_{mm} \sin(\theta_{cR} - \theta_m) - B_{mm} \cos(\theta_{cR} - \theta_m)) \quad (3.39)$$

Shunt converter:

$$P_{vR} = -V_{vR}^2 G_{vR} + V_{vR} V_k (G_{vR} \cos(\theta_{vR} - \theta_k) + B_{vR} \sin(\theta_{vR} - \theta_k)) \quad (3.40)$$

$$Q_{vR} = V_{vR}^2 B_{vR} + V_{vR} V_k (G_{vR} \sin(\theta_{vR} - \theta_k) - B_{vR} \cos(\theta_{vR} - \theta_k)) \quad (3.41)$$

Where

$$Y_{kk} = G_{kk} + jB_{kk} = Z_{cR}^{-1} + Z_{vR}^{-1} \quad (3.42)$$

$$Y_{mm} = G_{mm} + jB_{mm} = Z_{cR}^{-1} \quad (3.43)$$

$$Y_{km} = G_{km} + jB_{km} = -Z_{cR}^{-1} \quad (3.44)$$

$$Y_{vR} = G_{vR} + jB_{vR} = -Z_{vR}^{-1} \quad (3.45)$$

Assuming a loss free converter operation, the UPFC neither absorbs nor injects active power with respect to the AC system. The DC link voltage, V_{dc}, remains constant. The active power associated with the series converter becomes the DC power. The shunt converter must apply an equivalent amount of DC power to maintain V_{dc} constant. Hence the active power supplied to the shunt converter, must satisfy the active power demanded by the series converter,

$$P_{vR} + P_{cR} = 0 \quad (3.46)$$

3.2.2 UPFC JACOBIAN EQUATIONS

The state variables corresponding to the UPFC are combined with the network nodal voltage magnitudes and angles in a single frame-of-reference for a unified solution through a Newton-

Raphson method. The UPFC state variables are adjusted automatically so as to satisfy specified power flows and voltage magnitudes.

The UPFC linearized power equations are combined with the linearized system of equations corresponding to the rest of the network,

$$[F(x)] = [\mathrm{J}][\Delta \mathrm{X}] \tag{3.47}$$

Where,

$$\left[f\left(x\right)\right] = \left[\Delta P_k\ \Delta P_m\ \Delta Q_k\ \Delta Q_m\ \Delta P_{mk}\ \Delta Q_{mk}\ \Delta P_{bb}\right]^T \tag{3.48}$$

ΔP_{bb} is the power mismatch given by equation (3.46) and superscript T indicates the transposition. ΔX is the solution vector and J is the Jacobian matrix. The power mismatch equations are used as the guiding principle for conducting limit revisions. The mismatch provides an accurate indicator for determining the activation of limits revision for controllable device parameters. The revision criterion of the UPFC is based on its active power converter mismatch. For the case when the UPFC controls voltage magnitude at the AC shunt converter terminal (bus *k),* active power flowing from bus *m* to bus ***k*** and reactive power injected at bus ***m,*** and assuming that bus ***m*** is PQ-type, the solution vector and Jacobian matrix are,

$$\left[\Delta X\right] = \left[\Delta\theta_k\ \Delta\theta_m\ \frac{\Delta V_{vR}}{V_{vR}}\ \frac{\Delta V_m}{V_m}\ \Delta\theta_{cR}\ \frac{\Delta V_{cR}}{V_{cR}}\ \Delta\theta_{vR}\right]^T \tag{3.49}$$

$$[J] = \begin{bmatrix}
\frac{\partial P_k}{\partial \theta_k} & \frac{\partial P_k}{\partial \theta_m} & \frac{\partial P_k}{\partial V_{vR}}V_{vR} & \frac{\partial P_k}{\partial V_m}V_m & \frac{\partial P_k}{\partial \theta_{cR}} & \frac{\partial P_k}{\partial V_{cR}}V_{cR} & \frac{\partial P_k}{\partial \theta_{vR}} \\
\frac{\partial P_m}{\partial \theta_k} & \frac{\partial P_m}{\partial \theta_m} & 0 & \frac{\partial P_m}{\partial V_m}V_m & \frac{\partial P_m}{\partial \theta_{cR}} & \frac{\partial P_m}{\partial V_{cR}}V_{cR} & 0 \\
\frac{\partial Q_k}{\partial \theta_k} & \frac{\partial Q_k}{\partial \theta_m} & \frac{\partial Q_k}{\partial V_{vR}}V_{vR} & \frac{\partial Q_k}{\partial V_m}V_m & \frac{\partial Q_k}{\partial \theta_{cR}} & \frac{\partial Q_k}{\partial V_{cR}}V_{cR} & \frac{\partial Q_k}{\partial \theta_{vR}} \\
\frac{\partial Q_m}{\partial \theta_k} & \frac{\partial Q_m}{\partial \theta_m} & 0 & \frac{\partial Q_m}{\partial V_m}V_m & \frac{\partial Q_m}{\partial \theta_{cR}} & \frac{\partial Q_m}{\partial V_{cR}}V_{cR} & 0 \\
\frac{\partial P_{mk}}{\partial \theta_k} & \frac{\partial P_{mk}}{\partial \theta_m} & 0 & \frac{\partial P_{mk}}{\partial V_m}V_m & \frac{\partial P_{mk}}{\partial \theta_{cR}} & \frac{\partial P_{mk}}{\partial V_{cR}}V_{cR} & 0 \\
\frac{\partial Q_{mk}}{\partial \theta_k} & \frac{\partial Q_{mk}}{\partial \theta_m} & 0 & \frac{\partial Q_{mk}}{\partial V_m}V_m & \frac{\partial Q_{mk}}{\partial \theta_{cR}} & \frac{\partial Q_{mk}}{\partial V_{cR}}V_{cR} & 0 \\
\frac{\partial P_{bb}}{\partial \theta_k} & \frac{\partial P_{bb}}{\partial \theta_m} & \frac{\partial P_{bb}}{\partial V_m}V_{vR} & \frac{\partial P_{bb}}{\partial V_m}V_m & \frac{\partial P_{bb}}{\partial \theta_{cR}} & \frac{\partial P_{bb}}{\partial V_{cR}}V_{cR} & \frac{\partial P_{bb}}{\partial \theta_{vR}}
\end{bmatrix} \tag{3.50}$$

If the UPFC voltage control is deactivated, the third column of eqn. (3.50) is replaced by partial derivatives of the nodal and UPFC mismatch powers with respect to the nodal voltage magnitude V_k. Moreover, the shunt source voltage magnitude increment in eqn. (3.49), $\Delta V_{vR} / V_{vR}$, is replaced by the nodal voltage magnitude increment at bus *k*, $\Delta V_k / V_k$,. In this case, V_{vR} is maintained at a fixed value within prescribed limits, $V_{vRmin} \leq V_{vR} \leq V_{vRmax}$.

3.3 UPFC INITIAL CONDITIONS AND LIMIT REVISION

The solution of a nonlinear set of algebraic equations by a Newton-Raphson technique requires good starting conditions. In the load flow problem, experience has shown that for the case in which no controlled buses or branches are present, 1 p.u. voltage magnitude for all PQ buses and 0 voltage angles for all buses provide a suitable starting condition. For the UPFC, a set of equations which give good initial estimates can be obtained by assuming lossless UPFC and coupling transformers and null voltage angles in eqns. (3.34 - 3.37).

3.3.1 SERIES SOURCE INITIAL CONDITIONS

For specified nodal powers at bus *m*, the solution of eqns. (3.36) and (3.37) are:

$$\theta_{cR}^0 = \arctan\left(\frac{P_{mref}}{|C_1|}\right) \tag{3.51}$$

$$V_{cR}^0 = \left(\frac{X_{cR}}{V_m^{\,0}}\right)\sqrt{P_{mref}^2 + C_1^2} \tag{3.52}$$

Where

$$C_1 = Q_{mref} - \left(\frac{V_m^{\,0}}{X_{cR}}\right)(V_m^0 - V_k^0) \qquad \text{If} \quad V_m^0 \neq V_k^0 \tag{3.53}$$

$$C_1 = Q_{mref} \quad \text{If} \quad V_m^0 = V_k^0 \tag{3.54}$$

Where X_{cR} is the inductive reactance of the series source and subscript 0 indicated initial values.

3.3.2 SHUNT SOURCE INITIAL CONDITIONS

An equation for initializing the shunt voltage angle source can be obtained by substituting eqns. (3.38) and (3.40) into eqn. (3.46) and performing simple operations:

$$\theta_{vR} = -\arcsin\left(\frac{(V_k^0 - V_m^0)V_{cR}^0 X_{vR}\sin(\theta_{cR}^0)}{V_{vR}^0 V_k^0 X_{cR}}\right) \tag{3.55}$$

Where X_{vR} is the inductive reactance of the shunt source. When the shunt converter is acting as a voltage regulator, the voltage magnitude of the shunt source is initialized at the target voltage value and then it is updated at each iteration. Otherwise, if the shunt converter is not acting as a voltage regulator, the voltage magnitude of the shunt source is kept at a fixed value within prescribed limits, $V_{vRmin} \le V_{vR} \le V_{vRmax}$, for the whole iterative process.

3.3.3 LIMIT REVISION OF UPFC CONTROLLABLE VARIABLES

The mismatch provides an accurate indicator for determining the activation of limits revision for the controllable devices parameters. The revision criterion of the UPFC is based on its active power converter mismatch equation:

$$\Delta P_{bb}^i = P_{vR} + P_{cR} \tag{3.56}$$

Where i varies from 1 to the number of UPFCs. If a limit violation takes place in one of the voltage magnitudes of the UPFC sources, the voltage magnitude is fixed at that limit and the regulated variable is freed.

3.4 UPFC POWER FLOW IMPLEMENTATION

The proposed algorithm for solving a power flow problem embedded with UPFC is implemented by using the MATLAB software. The overall procedure of the proposed algorithm can be summarized as follows the input system data includes the basic system data needed for conventional power flow calculation, *i.e*., the number and types of buses, transmission line data, generation and load data, the location of UPFC, and the values of UPFC control parameters.

A) Algorithm of UPFC power flow

The following steps are implemented to perform UPFC power flow:

Step 1. Choose the initial values of the voltage magnitudes $|V|^{(0)}$ of all n_p load buses and $(n-1)$ angles $\delta^{(0)}$ of the voltages of all the buses except the slack bus.

Step 2. A dummy bus is created adjacent to shunt converter bus to facilitate the series converter connection through series transformer and initialize its voltage.

Step 3. Use the estimated $|V|^{(0)}$ and $\delta^{(0)}$ to calculate a total $n-1$ number of injected real power $P_{calc}{}^{(0)}$ and equal number of real power mismatch $\Delta P^{(0)}$.

Step 4. Use the estimated $|V|^{(0)}$ and $\delta^{(0)}$ to calculate a total n_p number of injected reactive power $Q_{calc}{}^{(0)}$ and equal number of reactive power mismatch $\Delta Q^{(0)}$.

Step 5. Use the estimated $|V|^{(0)}$ and $\delta^{(0)}$ to formulate the Jacobian matrix $J^{(0)}$.

Step 6. Modify Jacobian matrix and mismatch power equations to incorporate UPFC according to equations:

$$P_{vR} + P_{cR} = 0$$

$$[F(x)] = [\mathrm{J}][\Delta \mathrm{X}]$$

$$\left[f(x) \right] = \left[\Delta P_k \ \Delta P_m \ \Delta Q_k \ \Delta Q_m \ \Delta P_{mk} \ \Delta Q_{mk} \ \Delta P_{bb} \right]^T$$

$$[\Delta X] = \left[\Delta\theta_k \ \Delta\theta_m \ \frac{\Delta V_{vR}}{V_{vR}} \ \frac{\Delta V_m}{V_m} \ \Delta\theta_{cR} \ \frac{\Delta V_{cR}}{V_{cR}} \ \Delta\theta_{vR} \right]^T$$

$$[J] = \begin{bmatrix}
\frac{\partial P_k}{\partial \theta_k} & \frac{\partial P_k}{\partial \theta_m} & \frac{\partial P_k}{\partial V_{vR}} V_{vR} & \frac{\partial P_k}{\partial V_m} V_m & \frac{\partial P_k}{\partial \theta_{cR}} & \frac{\partial P_k}{\partial V_{cR}} V_{cR} & \frac{\partial P_k}{\partial \theta_{vR}} \\
\frac{\partial P_m}{\partial \theta_k} & \frac{\partial P_m}{\partial \theta_m} & 0 & \frac{\partial P_m}{\partial V_m} V_m & \frac{\partial P_m}{\partial \theta_{cR}} & \frac{\partial P_m}{\partial V_{cR}} V_{cR} & 0 \\
\frac{\partial Q_k}{\partial \theta_k} & \frac{\partial Q_k}{\partial \theta_m} & \frac{\partial Q_k}{\partial V_{vR}} V_{vR} & \frac{\partial Q_k}{\partial V_m} V_m & \frac{\partial Q_k}{\partial \theta_{cR}} & \frac{\partial Q_k}{\partial V_{cR}} V_{cR} & \frac{\partial Q_k}{\partial \theta_{vR}} \\
\frac{\partial Q_m}{\partial \theta_k} & \frac{\partial Q_m}{\partial \theta_m} & 0 & \frac{\partial Q_m}{\partial V_m} V_m & \frac{\partial Q_m}{\partial \theta_{cR}} & \frac{\partial Q_m}{\partial V_{cR}} V_{cR} & 0 \\
\frac{\partial P_{mk}}{\partial \theta_k} & \frac{\partial P_{mk}}{\partial \theta_m} & 0 & \frac{\partial P_{mk}}{\partial V_m} V_m & \frac{\partial P_{mk}}{\partial \theta_{cR}} & \frac{\partial P_{mk}}{\partial V_{cR}} V_{cR} & 0 \\
\frac{\partial Q_{mk}}{\partial \theta_k} & \frac{\partial Q_{mk}}{\partial \theta_m} & 0 & \frac{\partial Q_{mk}}{\partial V_m} V_m & \frac{\partial Q_{mk}}{\partial \theta_{cR}} & \frac{\partial Q_{mk}}{\partial V_{cR}} V_{cR} & 0 \\
\frac{\partial P_{bb}}{\partial \theta_k} & \frac{\partial P_{bb}}{\partial \theta_m} & \frac{\partial P_{bb}}{\partial V_m} V_{vR} & \frac{\partial P_{bb}}{\partial V_m} V_m & \frac{\partial P_{bb}}{\partial \theta_{cR}} & \frac{\partial P_{bb}}{\partial V_{cR}} V_{cR} & \frac{\partial P_{bb}}{\partial \theta_{vR}}
\end{bmatrix}$$

Step 7. Choose initial conditions for series and shunt converter parameters of UPFC using equations:

$$\theta_{cR}^{0} = \arctan\left(\frac{P_{mref}}{|C_1|}\right)$$

$$V_{cR}^{0} = \left(\frac{X_{cR}}{V_m^{\ 0}}\right)\sqrt{P_{mref}^2 + C_1^2}$$

$$\theta_{vR} = -\arcsin\left(\frac{(V_k^0 - V_m^0)V_{cR}^0 X_{vR}\sin(\theta_{cR}^0)}{V_{vR}^0 V_k^0 X_{cR}}\right)$$

Step 8. Apply power mismatch equation for limit revision of controllable parameters of UPFC.

$$\Delta P_{bb}^{i} = P_{vR} + P_{cR}$$

Step 9. Update the system bus bar voltages and check for convergence.

Step10. If the convergence is obtained within permissible limit then terminate the process and display the output power flow information. Otherwise, go back to step-6 to start the next iteration.

B) Flow Chart of UPFC Power Flow

The implementation of this model has been explained in the form of flow chart given in Fig. 3.2. In the flow chart, a step wise explanation of incorporating UPFC into power flow solution has been described on next page.

The system admittance matrix and the conventional Jacobian matrix are formed due to incoming of UPFC. At the next step, the Jacobian matrix is modified and power equations are mismatched. Then busbar voltages are updated at each iteration. Convergence is checked, whether achieved or not. If no, the Jacobian matrix is modified and the power equations are mismatched until convergence is achieved. If yes, the power flow results are displayed.

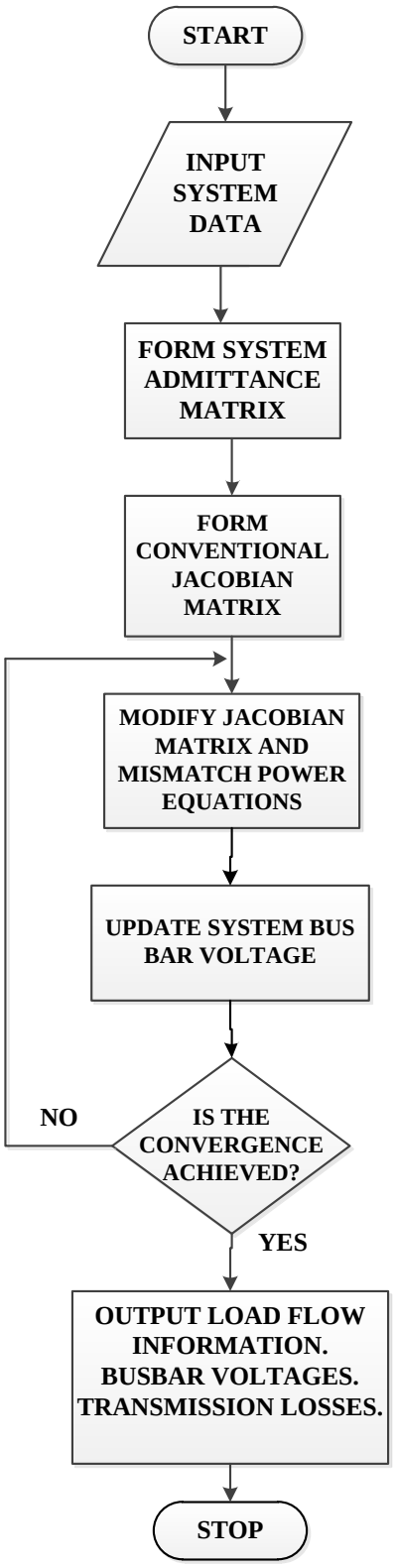

Fig. 3.2: Flow Chart of UPFC Power Flow

CHAPTER - 4

RESULTS AND DISCUSSION

4.1 SYSTEM SPECIFICATION AND BASE CASE SOLUTION

This chapter presents the results obtained on the performance of power system with incorporation of UPFC in the network. The performance has been studied on 5-Bus test system and the system is shown in Fig.4.1.

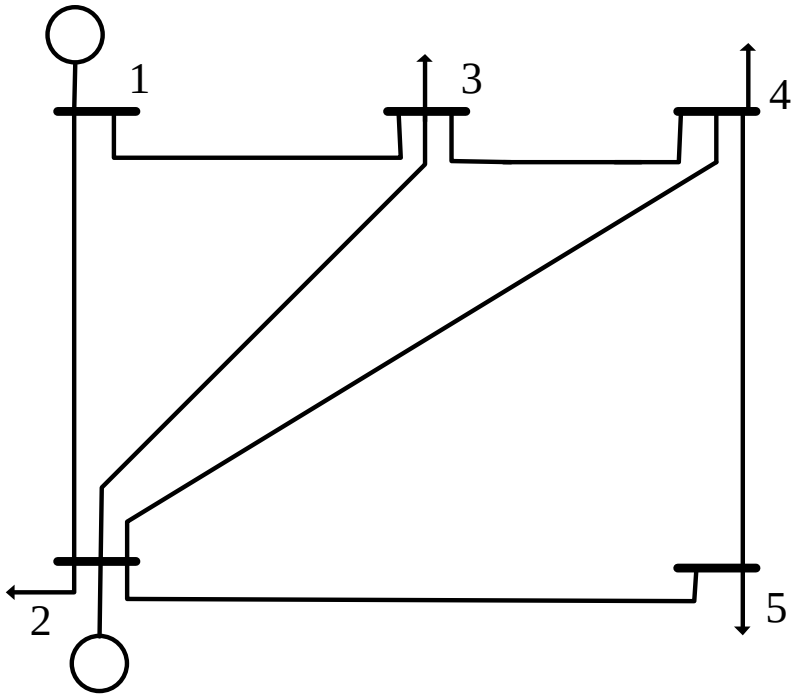

Fig. 4.1: 5-Bus Test System

First, the Newton- Raphson Algorithm is implemented on the 5-Bus test system [18] with the following parameters taken into consideration:

Base MVA = 100

Maximum number of Iterations = 100

Tolerance = 10^{-12}

The 5-Bus test system bus data and line data is shown in Table 4.1 and Table 4.2 respectively.

Table 4.1: Bus Data of 5-Bus Test System [18]

Bus No.	Bus Voltage (p.u.)	Voltage Angle(θ)	Generation		Load	
			MW	MVAR	MW	MVAR
1	1.06	0	0	0	0	0
2	1.0	0	40	30	20	10
3	1.0	0	0	0	45	15
4	1.0	0	0	0	40	5
5	1.0	0	0	0	60	10

Sending Bus (p)	Receiving Bus (q)	Impedance (Z_{pq})	Line Charging Susceptance ($Y'_{pq}/2$)
1	2	0.02+j0.06	0.0+j0.030
1	3	0.08+j0.24	0.0+j0.025
2	3	0.06+j0.18	0.0+j0.020
2	4	0.06+j0.18	0.0+j0.020
2	5	0.04+j0.12	0.0+j0.015
3	4	0.01+j0.03	0.0+j0.010
4	5	0.08+j0.24	0.0+j0.025

The power flow problem of 5-Bus test system when solved through Newton-Raphson method takes 6 iterations to converge. The table 4.3 shows nodal voltages and voltage angles of all the buses of the 5-bus system network after convergence. The nodal voltages and voltage angle values are within permissible limits.

The total system active power loss in the 5-Bus test system without UPFC is 6.52 MW. The line flow analysis of the test bus system without UPFC is shown in table 4.4.

Table 4.3: Nodal Voltages and Voltage angles without UPFC

Complex Voltages	**System Bus**				
	1	**2**	**3**	**4**	**5**
V (p.u)	1.06	1.00	0.9872	0.9841	0.9717
θ (deg.)	0	-2.0612	-4.6367	-4.9570	-5.7649

Table 4.4: Line Flow Analysis without UPFC

Line No.	**Sending End Bus**	**Receiving End Bus**	**Sending End**		**Receiving end**	
			P (MW)	**Q (MVAR)**	**P(MW)**	**Q(MVAR)**
1	1	2	89.33	74.00	-85.85	-72.91
2	1	3	41.79	16.82	-40.27	-17.51
3	2	3	24.47	-2.52	-24.11	-0.35
4	2	4	27.71	-1.72	-27.25	-0.83
5	2	5	54.66	5.56	-53.44	-4.83
6	3	4	19.39	2.86	-19.35	-4.69
7	4	5	6.60	0.52	-6.56	-5.17

4.2 EFFECT OF UPFC PLACEMENT

A small five- bus network has been used to show quantitavely, how the UPFC performs. We have modified the original network to include a UPFC which compensates the transmission line connected between bus-3 and bus-4 in Case-A and, between bus-4 and bus-5 for Case-B. This is shown in Fig. 4.2 and Fig. 4.3 respectively. Initial conditions of UPFC voltage sources are,

V_{vR} = 1 p.u., θ_{vR} = 0°, V_{cR}= 0.04 p.u., θ_{cR} = -87.0°. The series and shunt source impedance has values of $X_{cR} = X_{vR}$ = 0.1 p.u. A tight convergence in Case-I and Case-II was attained to a power mismatch tolerance of 10^{-12}. The UPFC upheld its target values.

A) Case – I

The modified 5-Bus test network with UPFC placed between bus-3 and bus-4 is shown in Fig. 4.2. A dummy bus is used to connect UPFC and is denoted by bus-6. The shunt converter of UPFC is set to regulate the voltage of bus-3 at 1 p.u. The series converter is connected at dummy bus-6.

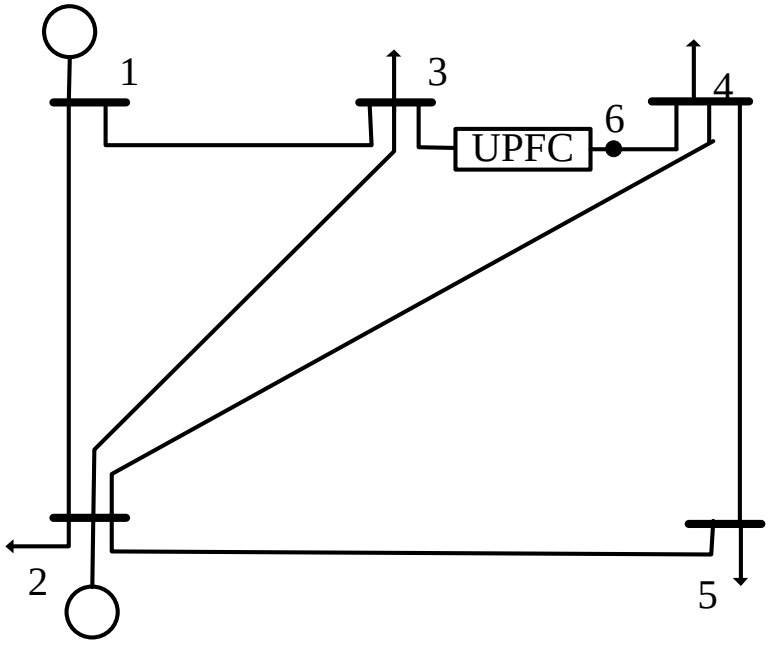

Fig. 4.2: Modified 5-Bus Test System for Case- I.

i) When target active and reactive power is at 40 MW and 2 MVAR respectively

The voltage magnitudes and voltage angles at all the bus when UPFC is incorporated between bus-3 and bus-4 is shown in table 4.5. After the convergence in five iterations, the UPFC sending end active and reactive power from bus-3 is 40 MW and -17.79 MVARs respectively. Also the target active and reactive power at dummy bus-6 is 40 MW and 2 MVARs. Moreover, the value of voltage sources of series and shunt converter are, V_{cR} = 0.1013 p.u, θ_{cR} = -92.7315°, V_{vR} = 1.0173 p.u, θ_{vR} = -6.0055°.

The total system active power loss in the 5-bus test system with UPFC between bus-3 and bus-4 is 6.48 MW. The line flow analysis of the test bus system with UPFC between bus-3 and bus-4 is shown in table 4.6.

Table 4.5: Nodal Voltages and Voltage angle for Case- I (UPFC between 3-4 bus) at target Active and Reactive power of 40 MW and 2 MVAR respectively

Complex Voltages	**System Bus**					
	1	**2**	**3**	**4**	**5**	**6**
V (p.u)	1.06	1.00	1.00	0.9917	0.9745	0.9965
θ (deg.)	0.0	-1.7693	-6.0161	-3.1906	-4.9741	-2.5122

Table 4.6: Line Flow Analysis for Case-I (UPFC between 3-4 bus) at target Active and Reactive power of 40 MW and 2 MVAR respectively

Line No.	**Sending End Bus**	**Receiving End Bus**	**Sending End Power**		**Receiving end Power**	
			P (MW)	**Q(MVAR)**	**P(MW)**	**Q(MVAR)**
1	1	2	81.14	76.42	-78.84	-75.88
2	1	3	50.34	9.34	-48.43	-8.92
3	2	3	37.48	-12.97	-36.57	11.71
4	2	4	13.74	-1.78	-13.63	-1.85
5	2	5	47.61	5.14	-46.69	-5.29
6	4	5	13.46	0.34	-13.31	-4.71
7	6	4	40.0	2.0	-39.84	-3.49

ii) When target active and reactive power is at 20 MW and 1 MVAR respectively

The voltage magnitudes and voltage angles at all the bus when UPFC is incorporated between bus-3 and bus-4 is shown in table 4.7. After the convergence in five iterations, the UPFC sending end active and reactive power from bus-3 is 20 MW and -9.42 MVARs respectively. Also the target active and reactive power at dummy bus-6 is 20 MW and 1 MVARs. Moreover, the value of voltage sources of series and shunt converter are, V_{cR} = 0.0299 p.u, θ_{cR} = -66.0379°, V_{vR} = 1.0103 p.u, θ_{vR} = -4.8397°.

The total system active power loss in the 5-bus test system with UPFC between bus-3 and bus-4 is 6.02 MW. The line flow analysis of the test bus system with UPFC between bus-3 and bus-4 is shown in table 4.8.

Table 4.7: Nodal Voltages and Voltage angle for Case- I (UPFC between 3-4 bus) at target Active and Reactive power of 20 MW and 1 MVAR respectively

Complex Voltages	**System Bus**					
	1	**2**	**3**	**4**	**5**	**6**
V (p.u)	1.06	1.00	1.00	0.9821	0.9710	0.9847
θ (deg.)	0.0	-2.0471	-4.8576	-4.8591	-5.7256	-4.5153

Table 4.8: Line Flow Analysis for Case-I (UPFC between 3-4 bus) at target Active and Reactive power of 20 MW and 1 MVAR respectively

Line No.	**Sending End Bus**	**Receiving End Bus**	**Sending End Power**		**Receiving end Power**	
			P (MW)	**Q(MVAR)**	**P(MW)**	**Q(MVAR)**
1	1	2	88.94	74.11	-86.46	-73.05
2	1	3	42.09	11.25	-40.68	-12.35
3	2	3	24.72	-9.57	-24.32	6.77
4	2	4	27.27	-0.49	-26.82	-2.10
5	2	5	54.47	6.17	-53.26	-5.45
6	4	5	6.78	-0.09	-6.74	-4.55
7	6	4	20.0	1.0	-19.96	-2.81

B) Case – II

The modified 5-Bus test network with UPFC placed between bus-4 and bus-5 is shown in Fig. 4.3. The shunt converter of UPFC is set to regulate the voltage of bus-4 at 1 p.u. A dummy bus is placed between bus-4 and bus-5 to connect UPFC and is denoted by bus-6. The series converter is connected at dummy bus-6.

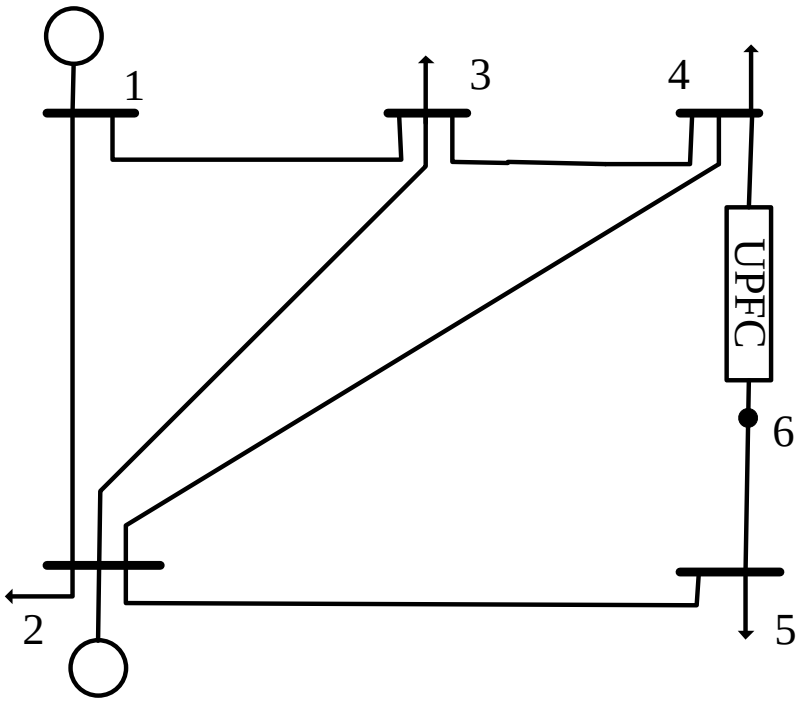

Fig. 4.3: Modified 5-Bus Test System for Case- II

i) When target active and reactive power is at 40 MW and 2MVAR respectively

The voltage magnitudes and voltage angles at all the bus when UPFC is incorporated between bus-4 and bus-5 is shown in table 4.9. After the convergence in seven iterations, the UPFC sending end active and reactive power from bus-4 is 40 MW and -31.07 MVARs respectively. Also the target active and reactive power at dummy bus-6 is 40 MW and 2 MVAR's. Moreover, the value of voltage sources of series and shunt converter are, V_{cR} = 0.1947 p.u, θ_{cR} = -98.6825°, V_{vR} = 1.0270 p.u, θ_{vR} = -6.7466°.

The total system active power loss in the 5-bus test system with UPFC between bus-4 and bus-5 is 7.88 MW. The line flow analysis of the test bus system with UPFC between bus-4 and bus-5 is shown in table 4.10.

The losses are high when UPFC is placed in between bus-4 and bus-5 when compared to base case power flow. However, UPFC is found effective to control voltage at bus-4 and regulate the line flow in line between bus-4 and bus-5 to the level as specified.

Table 4.9: Nodal Voltages and Voltage angles for Case- II (UPFC between 4-5 bus) at target Active and Reactive power of 40 MW and 2 MVAR respectively

Complex Voltages	System Bus					
	1	2	3	4	5	6
V (p.u)	1.06	1.00	0.9995	1.00	0.9847	1.0227
θ (deg.)	0.0	-1.8356	-5.9455	-6.6883	-3.1971	-2.0620

Table 4.10: Line Flow Analysis for Case-II (UPFC between 4-5 bus) at target Active and Reactive power of 40 MW and 2 MVAR respectively

Line No.	Sending End Bus	Receiving End Bus	Sending End Power		Receiving end Power	
			P (MW)	Q(MVAR)	P(MW)	Q(MVAR)
1	1	2	83.0	75.87	-80.66	-75.21
2	1	3	49.88	9.65	-48.0	-9.31
3	2	3	36.33	-12.41	-35.47	10.98
4	2	4	42.89	-14.31	-41.70	13.89
5	2	5	21.44	4.32	-21.24	-6.68
6	3	4	38.47	-16.67	-38.30	12.17
7	6	5	40.0	2.0	-38.76	-3.32

ii) When target active and reactive power is at 20 MW and 1 MVAR respectively

The voltage magnitudes and voltage angles at all the bus when UPFC is incorporated between bus-4 and bus-5 is shown in table 4.11. After the convergence in six iterations, the UPFC sending end active and reactive power from bus-4 is 20 MW and -22.60 MVARs respectively. Also the target active and reactive power at bus-5 is 20 MW and 1 MVARs. Moreover, the value of voltage sources of series and shunt converter are, V_{cR} = 0.0851 p.u, θ_{cR} = -94.9711°, V_{vR} = 1.0223 p.u, θ_{vR} = -5.7860°.

The total system active power loss in the 5-bus test system with UPFC between bus-4 and bus-5 is 6.39 MW. The line flow analysis of the test bus system with UPFC between bus-4 and bus-5 is shown in table 4.12.

Table 4.11: Nodal Voltages and Voltage angles for Case- II (UPFC between 4-5 bus) at target Active and Reactive power of 20 MW and 1 MVAR respectively

Complex Voltages	System Bus					
	1	2	3	4	5	6
V (p.u)	1.06	1.00	0.9998	1.00	0.9779	1.0012
θ (deg.)	0.0	-1.9559	-5.2656	-5.7859	-4.7069	-2.0610

Table 4.12: Line Flow Analysis for Case-II (UPFC between 4-5 bus) at target Active and Reactive power of 20 MW and 1 MVAR respectively

Line No.	Sending End Bus	Receiving End Bus	Sending End Power		Receiving end Power	
			P (MW)	Q(MVAR)	P(MW)	Q(MVAR)
1	1	2	86.38	74.87	-83.96	-73.98
2	1	3	45.01	10.65	-43.44	-11.24
3	2	3	29.17	-10.68	-28.62	8.35
4	2	4	33.77	-12.02	-33.03	10.25
5	2	5	41.01	4.21	-40.33	-5.09
6	3	4	27.06	-12.11	-26.97	7.35
7	6	5	20.0	1.0	-19.67	-4.91

4.3 EFFECT OF CONVERTER REACTANCE

The effect of converter source impedances on the UPFC final parameters were carried out using the network shown in Fig. 4.2. The UPFC is set to control voltage magnitude and active and reactive power flows at the same values as those specified in Section 4.2, Case I, subcase (i). The UPFC parameters corresponding to different combinations of source impedances are presented in table 4.13.

The parameters of the series source are only affected by its impedance value and they are independent of the shunt source reactance. Similarly the parameters of shunt source are only affected by the shunt source reactance. This can be observed in table 4.13 where by varying

series source impedances, change in series source parameters occurs while shunt source parameters remain unchanged. Similarly by varying shunt source impedance; there is a change in shunt source parameters only.

Table 4.13: Effect of UPFC Impedances

Impedances		Series Source		Shunt Source	
X_{cR}	X_{vR}	V_{cR}	θ_{cR}	V_{vR}	θ_{vR}
0.10	0.10	0.1013	-92.7315	1.0173	-6.0055
0.10	0.05	0.1013	-92.7315	1.0087	-6.0107
0.10	0.01	0.1013	-92.7315	1.0017	-6.0150
0.05	0.10	0.0812	-92.0775	1.0173	-6.0055
0.05	0.05	0.0812	-92.0775	1.0087	-6.0107
0.05	0.01	0.0812	-92.0775	1.0017	-6.0150
0.01	0.10	0.0651	-91.2642	1.0173	-6.0055
0.01	0.05	0.0651	-91.2642	1.0087	-6.0107
0.01	0.01	0.0651	-91.2642	1.0017	-6.0150

4.4 EFFECT OF INITIAL CONDITIONS

To show the impact of good initial conditions upon convergence, different series voltage source initial conditions were used. The UPFC is set to control voltage magnitude and active and reactive power flows at the same values as those specified in Section 4.2, Case – I, subcase (i).

Improper selection of initial conditions degrades Newton's quadratic convergence, and can increase the number of iterations for convergence as shown in table 4.14.

Also, there is no effect on nodal voltage magnitudes and voltage angles while varying initial conditions of the series voltage sources. The Complex nodal voltages for all bus are same as in table 4.5.

Table: 4.14: Effect of Initial Conditions

Initial Conditions		Iterations
V_{cR}	θ_{cR}	
0.25	10	16
0.01	-180	9
0.25	-30	8
0.06	-30	8
0.20	50	7
0.20	-90	5
0.04	-87	5
0.25	0	divergence

4.5 EFFECT OF NODAL VOLTAGE MAGNITUDE CONTROLLED BY SHUNT BRANCH

This section presents simulation results aimed at showing the effects of the UPFC when voltage magnitude controlled by shunt branch is varied. Two cases that are considered are:

A) When UPFC shunt converter regulates voltage magnitude at bus 3 and series converter is connected to dummy bus 6.

In this case, three different values of shunt converter voltage are taken into consideration and the simulated results are shown in tables given below. The Fig. 4.2 is considered for this analysis.

i) Voltage magnitude at 0.95 p.u.;

The table 4.15 shows the complex voltages for all the buses when the bus-3 voltage magnitude is regulated at 0.95 p.u. by the shunt converter branch. The convergence takes 6 iterations.

Table 4.15: Complex Voltages for Voltage magnitude at 0.95 p.u. for Case (A)

Complex Voltages	System Bus					
	1	**2**	**3**	**4**	**5**	**6**
V (p.u)	1.06	1.00	0.9500	0.9917	0.9745	0.9965
θ (deg.)	0.0	-1.7958	-5.3650	-3.2171	-5.0006	-2.5387

ii) Voltage magnitude at 1.0 p.u.;

Table 4.16: Complex Voltages for Voltage magnitude at 1.0 p.u. for Case (A)

Complex Voltages	System Bus					
	1	**2**	**3**	**4**	**5**	**6**
V (p.u)	1.06	1.00	1.00	0.9917	0.9745	0.9965
θ (deg.)	0.0	-1.7693	-6.0161	-3.1906	-4.9741	-2.5122

In this case the complex voltages for all buses are shown in table 4.16.

iii) Voltage magnitude at 1.05 p.u.;

Table 4.17: Complex Voltages for Voltage magnitude at 1.05 p.u. for Case (A)

Complex Voltages	System Bus					
	1	**2**	**3**	**4**	**5**	**6**
V (p.u)	1.06	1.00	1.05	0.9917	0.9745	0.9965
θ (deg.)	0.0	-1.7719	-6.7151	-3.1933	-4.9767	-2.5148

The Complex Voltages is shown in table 4.17 for the case when voltage magnitude at bus-3 is regulated at 1.05 p.u. by shunt converter branch.

Table 4.18: Effect of Voltage Magnitude controlled by Shunt Branch on UPFC parameters for case (A)

Case	Series Source			Shunt Source		
	V_{cR}	θ_{cR}	Q_{cR}	V_{vR}	θ_{vR}	Q_{vR}
I	0.1002	-122.2683	3.59	0.9208	-5.4842	-26.91
II	0.1013	-92.7315	4.07	1.0173	-6.0055	17.64
III	0.1268	-69.9396	4.60	1.100	-6.6079	55.0

The table 4.18 shows the effects on UPFC parameters when the voltage magnitude of bus-3 is varied by shunt branch. The results of the UPFC parameters are within permissible range.

B) When UPFC shunt converter regulates voltage magnitude at bus 4 and series converter is connected to bus 3.

In this case, three different values of shunt converter voltages are taken into consideration and the simulated results are shown in tables given below.

i) Voltage magnitude at 0.95 p.u.;

Table 4.19: Complex Voltages for Voltage magnitude at 0.95 p.u. for Case (B)

Complex Voltages	System Bus					
	1	2	3	4	5	6
V (p.u)	1.06	1.00	1.0168	0.950	0.9585	1.0261
θ (deg.)	0.0	-2.9966	-1.8339	-10.2461	-8.1512	-1.1888

The table 4.19 shows the complex voltages for all the buses when the bus-4 voltage magnitude is regulated at 0.95 p.u. by the shunt converter branch.

ii) Voltage magnitude at 1.0 p.u.

Table 4.20: Complex Voltages for Voltage magnitude at 1.0 p.u. for Case (B)

Complex Voltages	System Bus					
	1	**2**	**3**	**4**	**5**	**6**
V (p.u)	1.06	1.00	1.0168	1.00	0.9753	1.0261
θ (deg.)	0.0	-3.0054	-1.8388	-10.8949	-8.3630	-1.1937

The Complex Voltages is shown in table 4.20 for the case when voltage magnitude at bus-4 is regulated at 1.0 p.u. by shunt converter branch.

iii) Voltage magnitude at 1.05 p.u.

Table 4.21: Complex Voltages for Voltage magnitude at 1.05 p.u. for Case (B)

Complex Voltages	System Bus					
	1	**2**	**3**	**4**	**5**	**6**
V (p.u)	1.06	1.00	1.0168	1.05	0.9920	1.0215
θ (deg.)	0.0	-3.0606	-1.8696	-11.6272	-8.6501	-1.2244

The Complex Voltages is shown in table 4.21 for the case when voltage magnitude at bus-4 is regulated at 1.05 p.u. by shunt converter branch.

Table 4.22: Effect of Voltage Magnitude controlled by Shunt Branch on UPFC parameters for case (B)

Case	Series Source			Shunt Source		
	V_{cR}	θ_{cR}	Q_{cR}	V_{vR}	θ_{vR}	Q_{vR}
I	0.200	-115.5290	5.87	0.9482	-10.4352	-1.66
II	0.200	-101.5143	5.56	1.0385	-10.9541	39.94
III	0.200	-88.0119	2.02	1.10	-11.5881	55.0

The table 4.22 shows the effects on UPFC parameters when the voltage magnitude of bus-4 is varied by shunt branch. The results of the UPFC parameters are within permissible range.

CHAPTER-5

CONCLUSIONS AND SCOPE FOR FUTURE WORK

5.1 CONCLUSIONS

The present work on **"Power Flow Analysis with Unified Power Flow Controller"** has been carried out to analyze power flow solution of system comprising UPFC. The effect of placing UPFC between different buses is also analyzed by simulating comprehensive UPFC model in NR power flow method. The simulation has been carried out on 5-bus test system.

- The voltage magnitude of a bus can be regulated and stabilized by placing UPFC. The voltage of the bus associated with shunt converter is controlled at rated. With that the voltage profile of other buses also improved.
- The active and reactive power of a line can be controlled to desired level by placing UPFC appropriately.
- The power losses are not always reducing. However, the power losses can be reduced by suitably placing UPFC controller.

5.2 SCOPE OF FUTURE WORK

The study of a topic paves way for many other avenues related to this area of research. The following areas have been identified for future work:

- The analysis is carried out with only one UPFC at a time. The analysis can be extended to analyze the system with multiple FACTS devices.
- The cost of FACTS systems is significant and thus the allocation of FACTS devices can be implemented by considering practical cost of FACTS and the corresponding benefits carefully.

LIST OF PUBLICATIONS

- Adit Pandita, Sanjay K. Jain, "A Review on Power Flow Analysis with UPFC and its Applicability", *International Journal of Engineering Research & Technology (IJERT)*, Vol. 2, Issue 6, June – 2013.

REFERENCES

1. N. G. Hingorani and L. Gyugyi, “Understanding FACTS Concepts and Technology of Flexible AC Transmission Systems", *IEEE Press, Wiley- Interscience Publication*, 1999.

2. C. R. Fuerte-Esquivel and E. Acha, "Unified power flow controller: a critical comparison, of Newton-Raphson UPFC algorithms in power flow studies", *IEE Proc.-Gener. Transm. Distrib*, Vol. 144, No. 5, September 1997.

3. J. U. Lim and S. Moon, “UPFC Operation for the Minimization of Power Production and Delivery Costs”, *IEEE Power Engineering Society Meeting*, Vol. 1, Page 331-335, 2000.

4. H. Ambriz-Perez, E.Acha, C. R. Fuerte-Esquivel and A. De la Torre, “Incorporation of a UPFC model in an optimal power flow using Newton's method”, *IEE Proc.-Gener. Transm. Distrib*, Vol. 145, Issue 3, May 1998.

5. A. Nabavi-Niaki and M. R. Iravani, “Steady-state and Dynamic Models of Unified Power Flow Controller(UPFC) for Power System Studies”, *IEEE Transactions on Power Systems*, Vol. 11, No. 4, 2006.

6. C. R. Fuerte-Esquivel, E. Acha, and H. Ambriz-Perez, “A Comprehensive Newton-Raphson UPFC Model for the Quadratic Power Flow Solution of Practical Power Networks”, *IEEE Transactions on Power Systems*, Vol. 15, No. 1, February 2000.

7. G. Radman, R. S. Raje, “Power flow model/calculation for power systems with multiple FACTS controllers", *Electric Power Systems Research*, Volume 77, Issue 12, Page 1521-1531, , October 2007.

8. N. M. R. Santos, V. M. F. Pires and R. M. G. Castro, “A New Model to Incorporate Unified Power Flow Controllers in Power Flow Studies”, *IEEE PES Transmission and Distribution Conference and Exhibition*, Page 133-140, May 2006.

9. H. A. Abdelsalam, G. A. M. Aly, M. Abdelkrim, K. M. Shebl, “Optimal Location of Unified Power Flow Controller in Electrical Power Systems”, *Large Engineering systems Conference on Power Engineering*, Page 41-46, July 2004.

10. A. Farhangfar, S. J. Sajjadi and S. Afsharnia, “Power Flow Control and Loss Minimization with Unified Power Flow Control (UPFC)”, *Canadian Conference on Electrical and Computer Engineering,* Vol. 1, Page 385 – 388, 2004.

11. H. Chen, Y. Wang and R. Zhou, “Analysis of Voltage Stability Enhancement via Unified Power Flow Controller”, *International Conference on Power System Technology Proceedings PowerCon,* Vol.1, Page 403-408, 2000.

12. E. M. Yap, M. Al-Dabbagh and P. C. Thum, “Applications of FACTS Controller for Improving Power Transmission Capability*”, IEEE TENCON Region 10,* Page 1-6, 2005.

13. H. Mokhlis and K. M. Nor, “Implementation of UPFC model into Fast Decoupled Load Flow”, *IEEE Conference TENCON*, Vol. 3, Page 339-342, Nov. 2004.

14. S. N. Singh and I. Erlich, “Locating Unified Power Flow Controller for Enhancing Power System Loadability”, *International conference on Future Power Systems,* Page 5, 2005.

15. S. H. Kim, J. U. Lim and S. Moon, “Enhancement of Power System Security Level through the Power Flow Control of UPFC”, *IEEE Power Engineering Society Summer Meeting,* Vol. 1, Page 38-43, 2000.

16. H. I. Shaheen, G. I. Rashed, and S. J. Cheng, “Optimal Location and Parameters Setting of Unified Power Flow Controller Based on Evolutionary Optimization Techniques”, *IEEE Power Engineering Society General Meeting*, Page 1-8, 2007.

17. M. Noroozian, L. Angquist, M. Ghandhari and G. Andersson, “Use of UPFC for Optimal Power Flow”, *IEEE Transactions on Power Delivery,* Vol.12, No. 4, Page 1629-1634, 1997.

18. G. W. Stagg and A. H. El-Abiad, “Computer Methods in Power System Analysis”, *McGraw Hills Ltd. Publication,* 1968.

19. A. Berrizi, M. Delfanti, P. Marannino, M. S. Pasquadibisceglie and A. Silvestri, “Enhances Security Constrained OPF with FACTS Devices”, *IEEE Transactions on Power Systems,* Vol. 20, No. 3, August 2005.

20. X. P. Zhang, C. Rehtanz and B. Pal, "Flexible AC Transmission Systems: Modelling and Control", *Springer-Verlag Publication*, 2005.

21. M. Mashayekh, A. Kazemi and S. Jadid, “A New Approach for Modelling of UPFC In Power Flow and Optimum Power Flow Studies”, *IEEE Conference on Industrial Electronics and Applications,* Page 1-6, 2006.

22. J. J. Grainger and W. D. Stevenson, Jr., "Power System Analysis", *Tata McGraw Hill Publication*, 1994.